Geranium lake pigments : the role of the synthesis on the structure and composition

1   **Geranium lake pigments: the role of the synthesis on the structure and composition**

2   Victoria Beltran[1,2]*, Andrea Marchetti[1,2]*, Steven De Meyer[1,2], Gert Nuyts[1,2], Karolien De Wael[1,2+]

3   [1]AXES research group, University of Antwerp, Groenenborgerlaan 171, 2020, Antwerp, Belgium

4   [2]NanoLab Center of Excellence, University of Antwerp, Groenenborgerlaan 171, 2020, Antwerp,
5   Belgium.

6   * These authors contributed equally to this work

7   + corresponding author: karolien.dewael@uantwerpen.be

8

9   **Abstract**

10   Eosin Y has an extraordinary capacity to form complexes with metallic elements, that have applications

11   in many different fields, from photovoltaics and photocatalysis to historical artists' pigments. To unravel

12   the complexes reactivity, it is essential to have a precise knowledge of their structure and composition,

13   as well as how these can be affected by the synthesis protocol, an often underestimated factor.

14   This manuscript presents a thorough investigation of the structure and composition of eosin Y complexes

15   based on Al and Pb, by FTIR, XRPD and Raman spectroscopy, with a particular focus on the effect of the

16   synthesis conditions. Results clearly show the change of the coordination mode in Pb complexes

17   depending on the protocol, while the structure of Al complexes remains stable. In both cases, the

18   formation of by-products was observed. Additionally, a detailed band assignment of the FTIR and Raman

19   spectra of eosin Y and Pb and Al complexes is described, providing interesting details such as the

20   interaction between the metallic ion and the xanthene moiety (chromophore). This is extremely

21   important for the analysis of historical paintings where eosin Y is bonded to metallic ions, as well as for

22   other materials in dye-sensitized solar cells, wastewater treatment or photocatalysis.

23   **Keywords:** eosin Y, geranium lakes, FTIR spectroscopy, Raman spectroscopy, materials synthesis

24

25   **1. Introduction**

26   In relation to its photochemical properties, eosin Y (2',4',5',7'-tetrabromofluorescein) has been

1   traditionally used as a phosphorescent probe or photosensitizer.[1,2] Lately, this specific xanthene dye, with

2   a vibrant red colour, is gaining attention due to its capacity to form complexes with metallic elements,

3   having applications in many different fields such as drugs detection[3,4], dye sensitized solar cells[5–7] or

4   artists' pigments[8,9].

5   Eosin Y complexes used as pigments in paintings are better known as geranium lakes. They were

6   synthesized for the first time in the 19th century and, according to literature, they typically include Pb or

7   Al ions (Pb-lakes and Al-lakes respectively). Thanks to their extraordinarily intense red hue, they rapidly

8   gained popularity as artists' pigments, finding their way into the palette of great masters such as Vincent

9   Van Gogh and Paul Gauguin.[10–14] However, when exposed to the environment, the vivid red tone of the

10   geranium lakes tends to fade, leaving a greyish material behind.[15–17] Such a degradation may lead to

11   severe changes in the appearance of paintings, with cultural, societal and economic implications as a

12   result. Understanding how these pigments degrade is the first capital step towards defining the

13   appropriate measures to protect these masterpieces, thus a task of maximum priority.

14   Although previous studies provided valuable insights about the degradation reactions, there are still open

15   questions regarding the precise reactivity of geranium lakes and the factors influencing it.[18–20] One of the

16   reasons for such discrepancies might be linked to differences in composition caused by changes in the

17   synthesis of these pigments. Thus, deciphering the link between synthesis and composition of these

18   pigments is essential to allow a reliable comparison between published data and future studies.

19   To synthesize geranium lakes, a solution of dianionic eosin Y is prepared and mixed with a metallic salt

20   to precipitate the complex. This protocol is generally followed, with some of the experimental

21   parameters, in particular the pH of the initial solution and the amount of metallic salt added, changing

22   from one paper to another.[20–23] Nonetheless, an influence of pH and metal concentration in the

23   synthesized products can be reasonably expected. Eosin Y is, in fact, a polyprotic acid (one phenolic group

24   and one carboxylic group where $pK_{a\text{-}COOH} > pK_{a\text{-}OH}$)[24], hence the protolytic species present in the solution

25   are strongly influenced by the pH. Additionally, it should be also kept in mind that different tautomers

1   can be found for each protolytic specie. The main tautomers are described in Figure 1. [24] In principle,

2   each protolytic specie may form different types of intermolecular bonds with the metallic ions, ultimately

3   leading to different products. In addition, changes in pH may also lead to the formation of by-products.

4   Excess Pb and Al ions can react with hydroxyl ions leading to the formation of precipitates, finally resulting

5   in the contamination of the pigment and influencing the overall reactivity. The extent and nature of this

6   contamination is evidently linked not only to the pH, but also to the amount of metal ions in solution.

7   According to the literature, the stability of the complexes is linked to the photosensitizing properties of

8   the precursor dye and to the lifetime/reactivity of its excited state.[2,19] Such properties are typically

9   affected by the microenvironment of the photosensitizer.[25] Hence, it is likely that the changes in the

10 structure of the complex and the overall composition of the pigment (i.e. presence of by-products formed

11 during the synthesis) play a role in its stability.

12 Previous research has given valuable insights on the chemical nature of geranium lakes depending on the

13 type (Pb or Al) and number (one or two) of metallic salts used, elucidating the formation of a bond

14 between the carboxylic acid group of eosin Y and the metal ion.[26] However, no systematic study exists on

15 the effect of different synthesis conditions on the eosin Y-metal coordination and the overall chemical

16 composition including the presence of by-products. A correlation between changes in the synthesis

17 method and the composition of geranium lakes has been previously hypothesized[27] but not yet proven.

18 A thorough characterization of the eosin Y-metal coordination and of the by-products formed during

19 geranium lakes synthesis under different conditions is therefore a first crucial step towards a better

20 understanding the eosin complexes reactivity.

21 To allow the analysis of a wide range of compounds and their inter- and intramolecular interactions,

22 Fourier transform infrared (FTIR) spectroscopy is first addressed in this paper. The interpretation of FTIR

23 spectra can be complex in molecules such as eosin Y and geranium lakes due to the presence of several

24 bands, sometimes overlapping. To overcome this limitation, this research started with a detailed

25 assignment of the FTIR bands to determine the spectral markers of each molecule Such fundamental task

was performed through the comparison of eosin Y, Al-lakes and Pb-lakes with molecules having similar structures, as well as with a range of reaction products appositely modifying specific functional groups. FTIR spectra have been complemented with Raman spectroscopy, allowing to corroborate the assignment proposed. Based on this meticulous assignment, a study of the spectral changes depending on the synthesis conditions has been performed, focusing in particular on bands shifts and on the identification of by-products.

Differences in the behaviour of Pb-lakes and Al-lakes are observed, with the former being much more sensitive to modifications of the synthesis protocol than the latter. Furthermore, the presence of Pb- or Al-containing by-products in the synthesized pigments is demonstrated for the first time, as well as their correlation with the synthesis protocol. In particular, lead carbonates were formed in Pb-lakes and amorphous basic aluminium was formed in Al-lakes. These products would alter the reactivity of the pigment, in particular when mixed with a binding media that contains fatty acids (such as drying oils) due to the formation of metal soaps, that compromises the integrity of paintings.[28]

Additionally, the proposed assignment of the FTIR and Raman bands from eosin Y and geranium lakes spectra provides a reference to detect its presence and identify possible modifications in their structure. The accurate characterization of the eosin Y complexes and by-products in geranium lakes discussed in this study revealed the interaction between the metal ion and the phenoxide ion, and thus the xanthene moiety, that will ultimately help to understand their reactivity. This is a fundamental insight for their conservation in paintings but relevant also for any other research field in which eosin Y complexes appear.

2. Experimental section

2.1. Reagents

To perform the band assignment, the spectrum of pure eosin Y (Sigma Aldrich, ~99% purity, ref. E4009) has been compared to that of rhodamine B (Sigma Aldrich, ≥95%, ref. R6626) and fluorescein (J&K

1   Scientific, 95%, ref. 916551).

2   To prepare the complexes (Figure 5, 6 and 7), pure eosin Y has been used. Solid eosin Y has been

3   solubilized in a solution of NaOH (Sigma Aldrich, 98%, ref. S5881) prepared at pH=12. If necessary,

4   additional NaOH or an acid (H_2SO_4 (Sigma Aldrich, 99.999%, ref. 339741) for the syntheses of Al-lakes and

5   CH_3COOH (Sigma Aldrich, ≥99.7%, ref. 695092) for the syntheses of Pb-lakes) has been added until

6   reaching the pH required (pH_i). Afterwards, the metallic salt has been slowly added to the solution to

7   form the complex. For Pb-lakes, $Pb(COOCH_3)_2 \cdot 3H_2O$ (Fluka, ref. 32306) has been employed. For Al-lakes

8   the results obtained with $AlCl_3 \cdot 6H_2O$ (Alfa Aesar, 99%, ref. A14437) and $Al_2(SO_4)_3 \cdot 18\ H_2O$ (Sigma Aldrich,

9   ≥98%, ref. 237086) have been compared.

10   Additional synthesis protocols have been tested (Figure S6 and S7) using eosin Y disodium salt (Sigma

11   Aldrich, ≥85 % ref. E6003). The specific conditions used in each case are mentioned in the literature cited

12   therein.

13

14   *2.2. FTIR spectroscopy*

15   FTIR spectra have been collected with a spectrometer Bruker Alpha II equipped with a DTGS detector.

16   Measurements have been collected in transmission mode using KBr (Sigma Aldrich, FTIR grade, ref.

17   221864) pellets. A total of 128 scans have been accumulated in each sample, using a resolution of 4 cm^-

18   ^{1} and a wavenumber range between 4000 to 400 cm^{-1}. All spectra showed have not been corrected in

19   order to avoid any kind of distortion.

20

21   *2.3. Raman spectroscopy*

22   Raman spectra (Figure 2, 4 and 5) have been collected with the micro-Raman spectrometer InVia

23   Renishaw equipped with a CCD detector. Measurements were performed with a 785 nm laser and a

24   50x/NA 0.5 magnification objective. For each spectra 50 seconds measurements were accumulated

25   during 4 acquisitions. The energy used was 1% to avoid sample degradation. All spectra showed have not

1   been corrected in order to avoid any kind of distortion.

2   The Raman spectra of the Pb by-products showed a broad band from fluorescence, therefore the Bruker

3   Bravo PSSERS spectrometer (Bruker Optik GMBH, Ettlingen, Germany) was used (Figure 8). This device is

4   equipped with two lasers (785 and 853 nm) with sequentially shifted excitation to suppress fluorescence.

5   Laser power level and time cannot be adjusted, but is reported to be <100 mW and less than 1 min for a

6   single analysis. Spectral range is 300–3200 cm^{-1} at 10–12 cm^{-1} resolution.

7

8   *2.4. X-Ray powder diffraction*

9   The X-ray powder diffraction (XRPD) measurements were performed in transmission mode using a

10 focused (0.3 mm x 0.3 mm) monochromatic Ag-Kα X-ray source (22 keV) operated at 50 kV and 0.88 mA

11 while the emerging diffraction signals were collected with a PILATUS 200K detector. Multiple points on

12 the powder surface were measured with an exposure time of 10 s per point. Calibration and integration

13 of the diffraction signals was performed using the XRPDUA software package.

14

15 **3. Results and discussion**

16 *3.1. Foundations of a robust FTIR and Raman analysis: thorough band assignment of eosin Y and eosin Y*

17 *complexes*

18 Eosin Y and the corresponding Pb and Al complexes present FTIR and Raman spectra with several bands

19 in overlapping spectral regions. Nonetheless, a reliable band assignment for Pb-lakes and Al-lakes is

20 required in order to obtain novel insights about their structure and its changes depending on the

21 synthesis conditions.

22 The first step to determine the band assignment of geranium lakes includes the in-depth interpretation

23 of the FTIR and Raman spectra from eosin Y, since its molecular structure is well known. In solid state,

24 eosin Y exists in two forms: lactone and quinoid (Figure 1) (the presence of the zwitterionic form is almost

25 negligible[24]). These forms share many functionalities, namely the xanthene rings, the hydroxyl and the

1   bromine groups, they only differ in the structure of the carboxylic group. Pure solid eosin Y is composed

2   mainly of lactone form with small amounts of quinoid form[29,30], while eosin Y complexes present only the

3   quinoid form since the metal is bonded through the carboxylic acid group.[26] Therefore, in order to

4   compare the spectra of eosin Y and geranium lakes, it is necessary to discriminate the bands specific to

5   the lactone and quinoid forms from the bands of the shared structures.

6
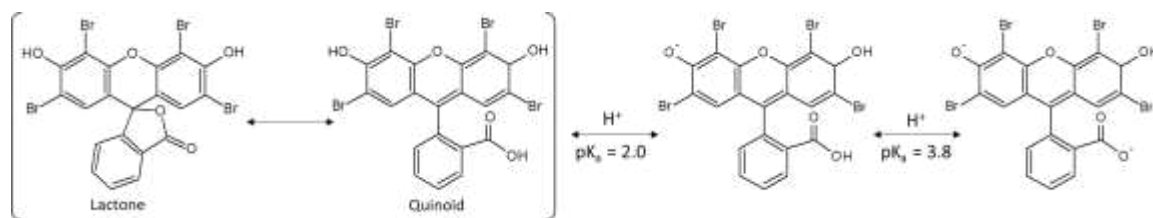
7

8   **Figure 1.** Main tautomers and pK$_a$ of eosin Y.

9

10   *3.1.1. Analysis of the structures shared in quinoid and lactone forms: comparative study of eosin Y,*

11   *rhodamine B and fluorescein*

12   In order to study the bands associated with the functionalities present in both quinoid and lactone forms,

13   the spectra of eosin Y has been compared to rhodamine B and fluorescein (Figure 2). Fluorescein can be

14   found in different forms: lactone, quinoid and zwitterionic, that can be distinguished by their colour and

15   their specific markers in the spectra (Figure S1). In this case the quinoid form has been used, which is

16   characterized by a strong red colour (unlike the zwitterionic form or the lactone form) and the lack of the

17   bands related to lactone or carboxylate groups. [31]

18   All molecules have a xanthene group (Figure 2, structure highlighted in green), hence the bands that are

19   present in all three spectra are linked to this functionality. The bands found only in eosin Y and fluorescein

20   spectra are probably linked to the hydroxyl, only found in these molecules (Figure 2, structure highlighted

21   in blue). Finally, the bands only found in the eosin Y spectra are related to the structures present just in

22   this molecule (Figure 2, structure highlighted in grey). The comparison of Raman and FTIR spectra, which

1   have different active vibrations, helped to verify the proposed assignment.

2
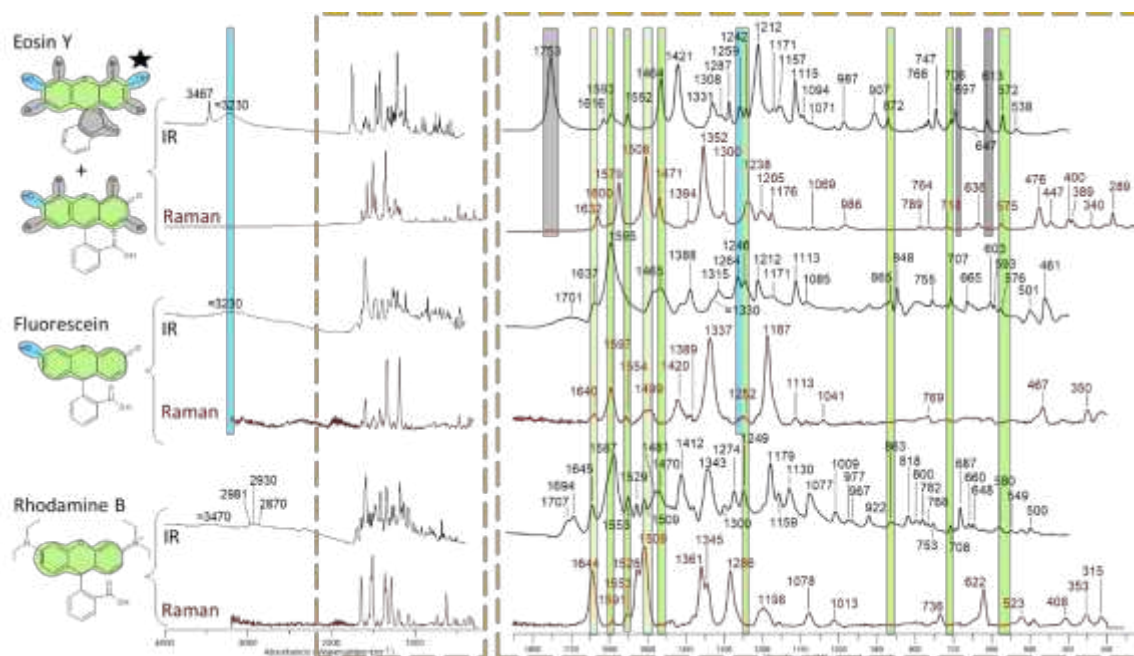
3

4   **Figure 2**. Comparison of the IR and Raman spectra of different xanthene dyes eosin Y, fluorescein and
5   rhodamine B. The structure of each compound is showed at the left, the star indicates the predominant
6   form in eosin Y. The shared structures have been marked in pink, green and blue. The structures only
7   present in eosin Y are marked in grey. FTIR spectra is plotted in black lines, Raman spectra in dark red, a
8   magnification of the region marked in orange is displayed at the right. The bands related to each structure
9   are marked with the same colour (full areas for FTIR bands, stripped areas for Raman bands).

10

11   The xanthene moiety (Figure 2, structure marked in green) has aromatic groups and an ether. Regarding

12   the aromatic groups, the C=C stretchings have been identified in the region between 1650 to 1450 cm^{-1},

13   specifically the bands at ≈1590, ≈1553 and ≈1465 cm^{-1} (more intense in the FTIR spectra but in some cases

14   also visible in the Raman spectra) and at ≈1640 and ≈1505 cm^{-1} (more intense in the Raman spectra but

15   in some cases also visible in the FTIR spectra). The C-O-C stretching of the ether group is most probably

16   associated to the band at ≈1245 cm^{-1}, only noticeable in the FTIR spectra. Three additional bands at ≈865,

17   ≈706 and ≈575 cm^{-1} are present in the spectra of all the three compounds, related to skeletal vibrations

18   of the shared structure.[34,35] Indeed, similar bands also appear in the spectra of rhodamine 6G, having the

1   same xanthene moiety.[36] These assignments agrees with previous studies based in computational

2   chemistry[32,33]

3   Previous research has linked the small bands at ≈1330, 1171 and 1113 cm^{-1} in the fluorescein spectra,

4   with similar relative intensity, and only noticeable in the FTIR spectra, to the xanthene moiety.[31,37,38] In

5   the spectra of eosin Y and rhodamine B, bands in similar regions can be observed too, associated to the

6   same functional group. The band shifts observed in each spectrum (1331-1330-1343 cm^{-1}; 1171-1171-

7   1179 cm^{-1}; 1115-1113-1130 cm^{-1}) can be explained by the different substituents of the xanthene in each

8   molecule.

9   The bands related to the hydroxyl group (Figure 2, structures marked in blue) appear at ≈3230 cm^{-1}, linked

10   to the O-H stretching, and at ≈1260 cm^{-1}, linked to the C-O stretching / O-H deformation. Both bands are

11   only present in the FTIR spectra of eosin Y and fluorescein since this Raman vibration is weak. However,

12   some differences can be noticed in the O-H stretching region: the band from fluorescein is very broad

13   and there is an additional peak at 3467 cm^{-1} in the spectra of eosin Y. The broader band of fluorescein is

14   explained by the presence of two types of –OH (hydroxyls and carboxylic groups), each one forming

15   hydrogen bonds between them as well as with the ketone group: this wide range of interactions broadens

16   the band. On the other hand, eosin Y has only one type of –OH (hydroxyls) which, in addition, are less

17   prone to form hydrogen bonds due to the steric hindrance caused by the adjacent Br atoms. For this

18   reason, the band of bonded –OH (3230 cm^{-1}) is lower and narrower and there is also a peak at 3467 cm^{-1}

19   which is probably associated to the single-hydrogen bridges, that tend to appear in this region[39].

20   Finally, there are a few bands found only in the spectra of eosin Y (Figure 2, structures marked in grey).

21   The clearest example is located at 1753 cm^{-1}, related to the C=O stretching of the lactone group.[34,35]

22   Despite fluorescein and rhodamine B also contain carboxylic groups, the band related to the C=O

23   stretching is expected to appear at a much lower wavenumber, overlapped with the bands of aromatics.

24   This agrees with the higher intensity of the bands at 1597 and 1587 cm^{-1} in the spectra of fluorescein and

25   rhodamine B respectively, compared to the other bands related to the C=C stretching of the aromatic

1   groups. The decrease of the wavenumber is explained by the conjugation of the C=O bonds and the higher

2   number of intermolecular bonds of fluorescein and rhodamine B compared to eosin Y, whose –OH are

3   less available as a result of the steric hindrance due to the Br atoms. Both effects contribute to decrease

4   the wavenumber of the carbonyl peak.[34]

5   Additionally, there are two bands at 697 and 613 cm^{-1}, probably related to the C-Br stretching. Indeed,

6   the fact that these two bands are also present in the FTIR spectra of 2,6-dibromophenol, that contains

7   similar C-Br bonds, supports this hypothesis.[40]

8

9   *3.1.2. Discrimination of the bands specific to quinoid and lactone forms: comparative study based on the*

10   *reactivity of eosin Y*

11   In order to discriminate the bands related to lactone and quinoid forms, eosin Y has been mixed with

12   different solvents that modify the carboxylic group, monitoring the reactions by FTIR spectroscopy

13   (Figure 3). Raman spectroscopy has not been used here since most of the vibrations related to the

14   expected changes are not Raman active.[34,35] In detail, pure eosin Y has been treated with ethanol (Figure

15   3a) and with acetone (Figure 3b) to alter the lactone group. Additionally, eosin Y has been mixed with

16   water and filtered to isolate the non-soluble fraction, corresponding to the weakly-polar lactone form

17   (Figure 3c). The spectra of the modified compounds have been compared to pure eosin Y (i.e. mainly

18   lactone form with small amounts of quinoid form) (Figure 3d).

19   The expected reactivity has been verified by focusing on the spectral region corresponding to the C=O

20   stretching, where the changes are clear since there are no overlaps with bands related to other functional

21   groups. In particular, when the lactone group (Figure 3, structure highlighted in green) is modified

22   (spectra 3a and 3b), the intensity of the corresponding band centred at 1753 cm^{-1}, decreases compared

23   to pure eosin Y (spectrum 3d). After the reaction with ethanol (spectrum 3a) where the opening of the

24   lactone and the esterification of the carboxylic acid (Figure 3, structure highlighted in grey) is expected,

25   the band at 1753 cm^{-1} is broader. This is explained by the formation of the ester group, whose C=O

1   stretching typically appears around ≈1730 cm^{-1}.[34,35] After the reaction with acetone (spectrum 3b), where

2   the formation of the quinoid form is expected, two shoulders at ≈1703 and 1717 cm^{-1} appear. This change

3   is related to the occurrence of the carboxylic group, whose C=O stretching typically appears around ≈1700

4   cm^{-1} (Figure 3, structure highlighted in brown), and the ketone, whose C=O stretching appears normally

5   at ≈1717 cm^{-1} (Figure 3, structure highlighted in pink).[34,35] The ketone band is probably present also in

6   the spectrum 3a, but it is hidden by other more intense bands.

7   As it can be noticed, the C=O stretching related to the –COOH group from the quinoid form of eosin Y

8   appears at higher wavenumber than fluorescein and rhodamine B (Figure 2). Despite the C=O from all

9   three molecules being conjugated, eosin Y cannot form as many hydrogen bonds as fluorescein and

10   rhodamine B due to the steric hindrance of the –OH and ketone groups, which explains the higher

11   wavenumber from the eosin Y band.[34,35]

12   Conversely, the band at 1753 cm^{-1} in spectrum 3c (pure lactone form) is very narrow. This can be

13   explained by the presence of only one type of C=O. In spectrum 3d (pure eosin Y), the band at 1753 cm^{-1}

14   is broader than in 3c because pure eosin Y contains mainly lactone form but also small amounts of quinoid

15   form: quinoid form includes the C=O from both the carboxylic group and the ketone, so the related C=O

16   stretching bands overlap with the band at 1753 cm^{-1} making it broader.

17   Having confirmed the expected reactivity of eosin Y treated with different solvents by the band at 1753

18   cm^{-1}, the additional bands associated to these molecular changes can be identified. In particular, the

19   bands in the region below 1600 cm^{-1}, typically more overlapped, are I) C-O stretching / O-H deformation

20   of the carboxylic groups present in quinoid form, II) C=C stretching of the C=C bonds that appear in the

21   quinoid form and III) bands linked to the hydroxyl group that appear mostly in the lactone form.

22   I) Regarding the carboxylic groups, spectra 3a and 3b show a decrease of the relative intensity of the

23   band at ≈1212 cm^{-1} compared to other bands that do not change between lactone and quinoid form,

24   such as the ones at 1467 and 1422 cm^{-1}. This indicates the relationship of this and with the lactone form

25   (Figure 3, structures highlighted in green), probably C-O st / O-H deformation of the lactone group.

1   Indeed, this band is very small in fluorescein, where the lactone form is minor, and it is absent in

2   rhodamine B, where no lactones are present, which can be known by their strong colour[31,41] (Figure 2).

3   Similarly, the increase of the shoulder at ≈1185 and ≈1171 cm^{-1} can be noticed (spectra 3a and 3b

4   respectively), most likely related to the same type of vibrations but for the ester group (Figure 3, structure

5   highlighted in grey) and the carboxylic acid (Figure 3, structure highlighted in brown) formed.[34,35]

6
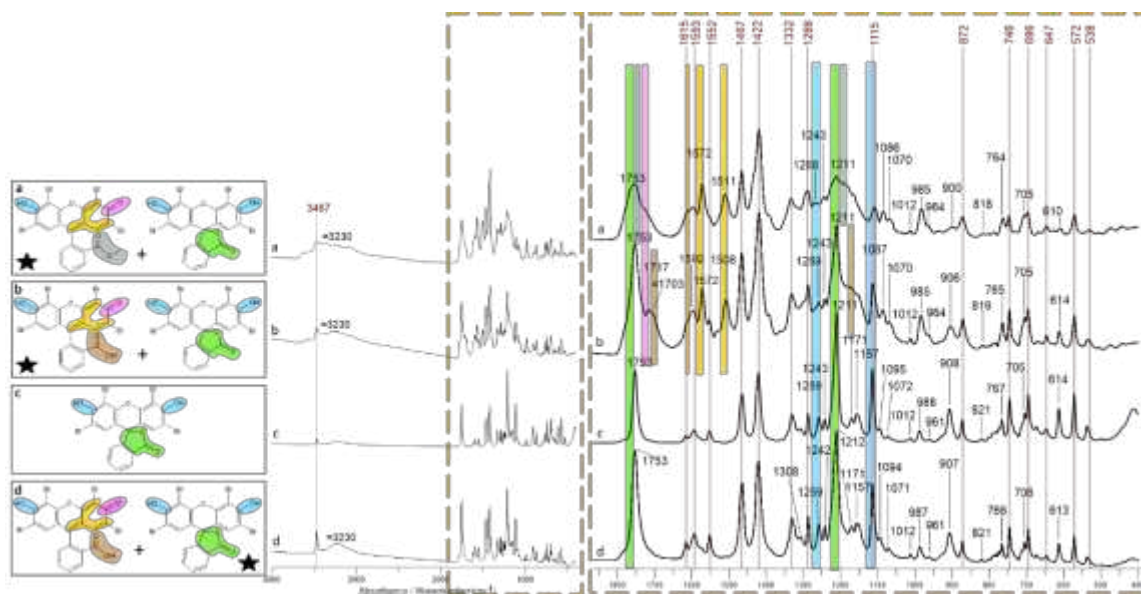
8   **Figure 3**. Reactivity of eosin Y with different solvents followed by FTIR spectroscopy. The structure(s) of
9   each sample is showed at the left a) eosin Y after reacting with ethanol, b) eosin Y after reacting with
10   acetone, c) fraction of eosin Y not soluble in water, d) eosin Y. The predominant molecule in each case is
11   marked with a star. The shared structures have been marked in the same colors that the associated bands
12   in the spectra. A magnification of the spectral region marked in orange is displayed at the right, the bands
13   written in red are present in all the samples.

14

15   II) Regarding the C=C bonds (Figure 3, structures highlighted in yellow), spectra 3a and 3b show an

16   increase of the bands at 1602, 1572 and ≈1510 cm^{-1}, presumably related to the C=C stretching of the new

17   C=C bonds formed.

18   III) Regarding the hydroxyl groups (Figure 3, structures highlighted in blue), the band at 1259 cm^{-1},

19   previously related to the –OH group, has slightly decreased in spectra 3a and 3b. Since the proportion of

1 –OH is lower in the quinoid structure (main form in spectra 3a and 3b), such a decrease is in good

2 agreement with the band assignment formerly stablished. In a similar fashion, a decrease of the band at

3 1115 cm^{-1} in spectra 3a and 3b is also noticeable, that could be explained by the contribution of the -OH

4 group to this band.

5 During the experiments of Figure 3 no changes in the ether, the skeletal vibrations and the C-Br bonds

6 are expected. As it can be seen, the bands previously associated to these functional groups are present

7 in all the spectra (although some of them are now overlapped by neighbouring bands), which

8 corroborates the stablished band assignment.

9

10 *3.1.3. Band assignment proposed for eosin Y and geranium lakes*

11 The results of the experimental approach previously discussed (Figures 2 and 3) complemented with

12 minor literature data[34,35], allowed to propose a novel band assignment for the FTIR and Raman spectra

13 from eosin Y. This exhaustive interpretation is displayed in Figure 4, (experimental assignments in blue,

14 assignments from literature in green).

15 Based on the band assignment of eosin Y and the bands related to its quinoid form, the FTIR and Raman

16 spectra of geranium lakes complexes have been proposed (Figure 5). $Al_2(SO_4)_3$ has been used to

17 synthesize Al-lakes, previous studies have reported indistinctively the use of $Al_2(SO_4)_3$[26] and $AlCl_3$[21,42],

18 indeed the FTIR and Raman spectra obtained for both compounds showed no significant differences

19 (Figure S2). The lakes have been obtained at pH_i=10 and 0.8 g of reagent ($Pb(COOCH_3)_2$) for Pb-lake and

20 pH_i=12.2 and 0.8 g of reagent ($AlCl_3$) for Al-lake in order to decrease the presence of by-products that

21 may interfere with the interpretation of the FTIR spectra. However, the effect of these parameters will

22 be discussed in the following sections. The spectra of the lakes have been compared to eosin Y disodium

23 salt, obtained from the solution of eosin Y before adding the metallic salt.

24
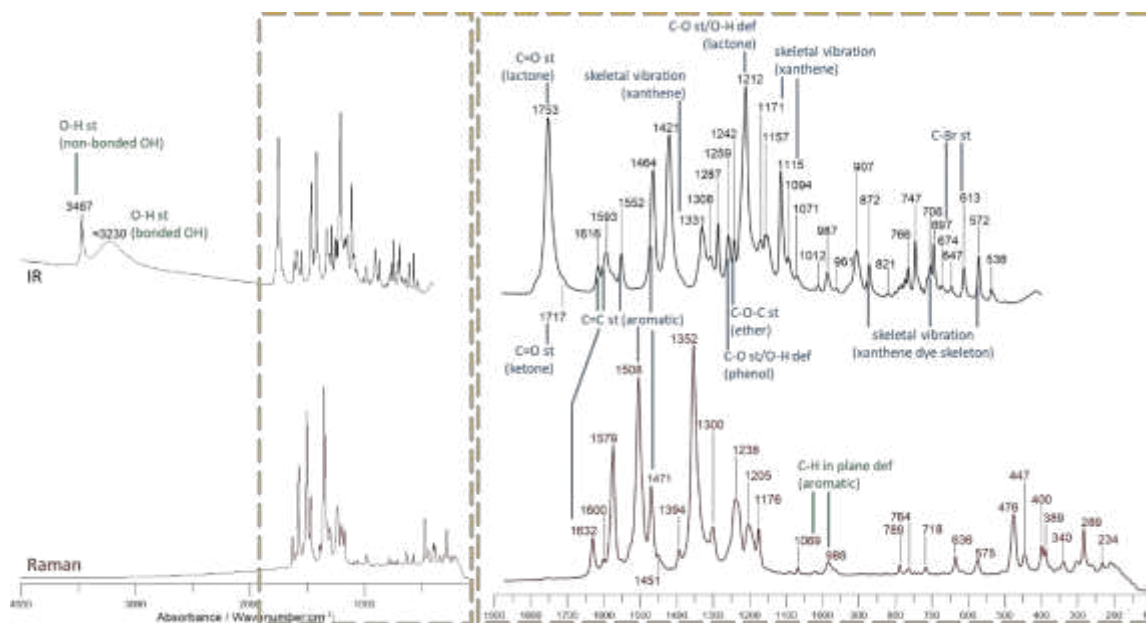
Figure 4. Eosin Y Raman and FTIR spectra with the proposed band assignment. Blue assignments are obtained from the comparisons of Figure 2 and 3. Green assignments are obtained from the literature. A magnification of the spectral region marked in orange is displayed at the right.

The first noticeable change in the FTIR spectra from both synthesized lakes and eosin Y disodium salt (Figure 5) is the decreasing/lack of the bands at 1753 and 1212 cm^{-1} related to lactone, due to the presence of the carboxylate group. This change confirms the relationship between these bands and the lactone group. Nevertheless, a small peak at 1753 cm^{-1} is still noticeable in the spectra of Pb-lake and Al-lake, demonstrating the presence of small amounts of eosin Y in lactone form in the products.

Compared to the eosin Y FTIR spectra, two new peaks at ≈1555 and ≈1445 cm^{-1} can be observed. These are probably linked to the C=O stretching, asymmetric and symmetric respectively, of the newly-formed carboxylate group. These bands are broad due to the overlapping with other smaller peaks from the C=C aromatic groups at ≈1570, ≈1510 and ≈1466 cm^{-1} previously mentioned. The presence of the C=C bands in the FTIR spectra is confirmed by the Raman spectra (Figure 5, red lines), where the C=O stretching vibrations are not active, and by their presence in the FTIR spectra a and b from Figure 3, related to the quinoid form of eosin Y. Previous works assigned other bands to the C=O stretching of the carboxylate group based on theoretical models[43], however carboxylate frequencies are influenced by many factors

14

1   therefore they difficult to predict[44]. Furthermore, the attribution of the ≈1555 and ≈1445 cm^{-1} to the

2   carboxylate group is additionally supported by three evidences: I) these vibrations are not active in

3   Raman, and no bands can be detected at these frequencies in the Raman spectra, II) small shifts can be

4   seen in the bands when different metals are bonded to eosin Y, which is explained by the differences in

5   the electronegativity of the metallic ions and in the type of coordination between the metal and the

6   ligand and III) the same carboxylate bands have been detected at similar frequencies (1600-1560 and

7   1400-1430 cm^{-1}) in the spectra of zwitterionic fluorescein.[31]

8
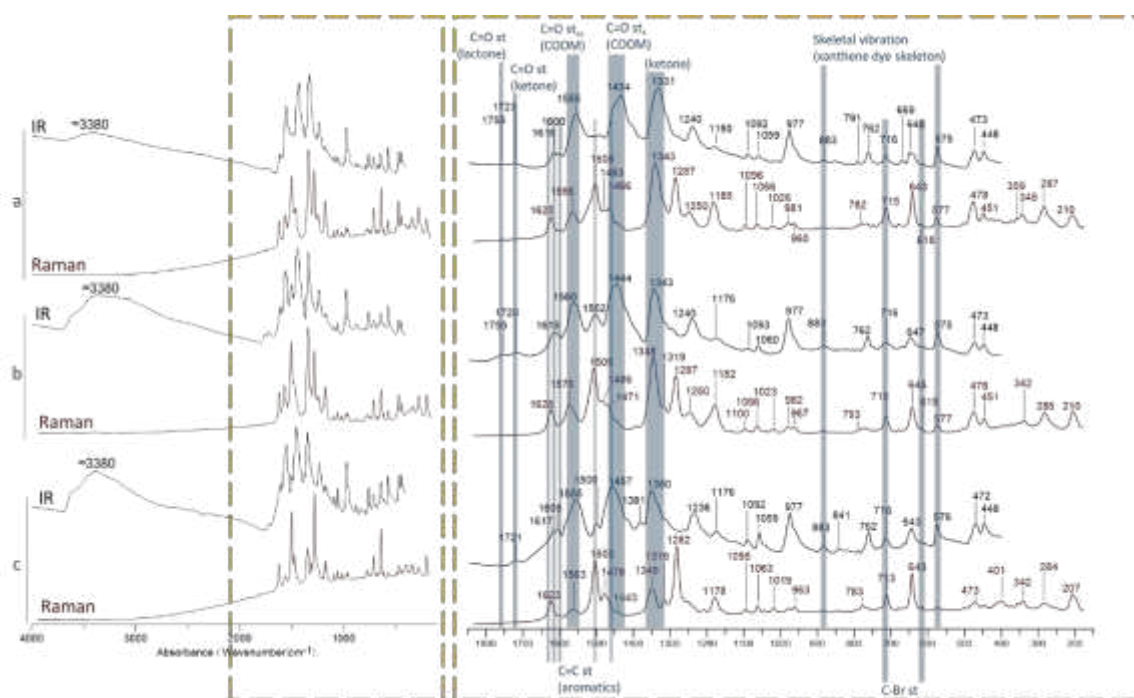
10 **Figure 5**. Raman and FTIR spectra and proposed band assignment from a) Pb- lake, b) Al-lake and c)
11 disodium salt of eosin Y. A magnification of the spectral region marked in orange is displayed at the right.

12

13 Another intense band, present in all the FTIR spectra of Figure 5, is the one at ≈1340 cm^{-1}. In addition,

14 small shifts in the position of this band are noticeable for the different compounds (1331, 1343 and 1350

15 cm^{-1}), in the same direction and with similar magnitude as the ones observed in the C=O symmetric

16 stretching of carboxylates (1434, 1444, 1457 cm^{-1} respectively). Consequently, we propose to assign this

1   band to the ketone interconverted with the deprotonated hydroxyl from the xanthene group (phenoxide

2   ion), which is interacting with the metallic ion of the complex causing those small shifts depending on the

3   electronegativity of the metal. The nature of the interaction between phenoxide ion and the metallic ion

4   is not certain, one hypothesis is the formation of a metallic chelate, whose asymmetric and symmetric

5   stretching use to fall between 1608-1524 cm^{-1} and 1390-1309 cm^{-1} respectively.[45] Thus, the asymmetric

6   stretching would be overlapped and only the symmetric stretching could be distinguished. As it has been

7   previously mentioned (Figure 2), this vibration would overlap the minor peak related to the xanthene

8   group at 1340 cm^{-1}. However, the contribution of the xanthene is expected to be very small here since,

9   as it has been previously noticed, its intensity is similar to the other bands related to this group at ≈1176

10   and ≈1115 cm^{-1}, which in this case are very low.

11   The assignment of the ≈1340 cm^{-1} band to the phenoxide ion interacting with the metallic ion is supported

12   by three evidences, namely I) the presence of a similar band in the FTIR spectra of deprotonated

13   fluorescein, which has been assigned to the oxygenated groups from the xanthene moiety [31,37], II) the

14   FTIR spectra of eosin B disodium salt (which contains Br and $-NO_2$ substituents in the xanthene rings [20]):

15   the additional $-NO_2$ group is expected to create an steric impediment that decreases the interactions of

16   phenoxide ion-metal, therefore the band has lower intensity and III) the interaction phenoxide ion-metal

17   has been already detected in eosin Y adsorbed in titania [46].

18   The interaction metal ion-phenoxide ion, and thus with the xanthene chromophore of the eosin Y

19   molecule, implies a potential influence of the metal on the properties of the fundamental and excited

20   states of the complex. Such an interaction is in agreement with the differences in colour experimentally

21   observed between Pb- and Al-lakes (Figure S3 and previous works[26,42]). Given the close connection

22   between light absorption, photosensitizing properties and stability of geranium lakes, this evidence might

23   also help explaining the differences in reactivity reported in literature for eosin Y complexes.[19,42,47]

24   On the other hand, the spectra of the synthesized products allow to corroborate some band assignments

25   previously proposed related to I) the aromatic groups (≈1616, ≈1600 and ≈1500 cm^{-1}), the skeletal

1   vibrations (≈880, ≈715 and ≈575 cm^{-1}) and the C-Br bonds (≈613 cm^{-1}) in the FTIR spectra and II) the

2   aromatic groups (≈1625, ≈1505 and ≈1470 cm^{-1}) in the Raman spectra. These groups are present in all

3   mentioned compounds, so the fact that these bands are present in all spectra confirms the band

4   assignment proposed.

5   The FTIR and Raman spectral markers of eosin Y and lakes have been summarized in **Table 1**. As it can be

6   seen, both techniques allow the discrimination of eosin Y from the synthesized compounds. On the

7   contrary, the Raman spectra from Al-lake, Pb-lake and eosin Y disodium salt are very similar, therefore

8   FTIR spectroscopy is a more suitable technique to distinguish them.

9

10   *3.2. Characterization of geranium lakes synthesized following different protocols*

11   Pb-lakes and Al-lakes are traditionally synthesized by first preparing a solution of dianionic eosin Y where

12   the metallic salt is then added[20–23]. For each type of lake, the synthesis was repeated changing either I)

13   the pH of the solution before adding the metallic salt (pH$_i$) with a fixed amount of metallic salt or II) the

14   amount of metallic salt added with a fixed pH$_i$. Since the pH affects the protolytic species of eosin Y

15   present in the solution and the formation of by-products, the pH after the addition of the metallic salt

16   was also measured (pH$_f$). The obtained geranium lakes have been analysed by means of FTIR

17   spectroscopy following the band assignment previously proposed. Raman spectroscopy has not been

18   used here since the changes are linked to the carboxylate group, for which the vibrations are more active

19   in the FTIR spectra. This allowed to systematically investigate potential changes in the lakes structure.

20   The yield was calculated according to the molecular formula previously proposed[26] considering eosin Y

21   as the limiting reagent. The obtained values are >100% meaning that the molecular formulas used do not

22   reflect the exact composition of the samples: since no other molecular formulas have been proposed,

23   these results have been displayed for the sake of comparison and labelled as "% of Obtained Product"

24   (%OP).

25

Eosin Y		Disodium salt of eosin Y		Pb-lake		Al-lake		Assignment
FTIR	Raman	FTIR	Raman	FTIR	Raman	FTIR	Raman	
1753 *1750[a]* *1753[b]* *1754[d]* *1747[e]*								C=O st (lactone)
		1457 *1453[a]* *1455[c]* *1458[f]*		1444		1434		C=O st_s (carboxylate)
		1350 *1352[c]* *1350[f]*		1343		1331		*probably related to ketone*
			1282		1287		1287	Skeletal vibration
1211 *1209[a]* *1215[d]*								C-O st/O-H def (lactone)
	1205							Skeletal vibration
1115 *1115[a]* *1113[e]*								Skeletal vibration (xanthene)
907 *906[e]*								Skeletal vibration (xanthene)
		472 *469[c]* *470[f]*		473		473		Skeletal vibration
		448 *447[f]*		448		448		Skeletal vibration
	400 *400[e]*		400					Skeletal vibration
	390							Skeletal vibration

Table 1. Specific markers of each compound in the FTIR and Raman spectra. The numbers in italics correspond to the precise values of these bands in previous works: a[26], b[48], c[20], d[43], e[49] and f[50].

It should be pointed out that, instead of using only one type of metallic salt, some historical recipes include another type of inorganic component in the synthesis (previous works[21,23,26] and references cited therein), that could be also coordinated to the eosin Y molecule forming the so called geranium bimetallic lakes, i.e. eosin Y coordinated to two types of metallic ions. However, since the analysis of the pigments produced following such recipes showed that eosin Y is coordinated to only one type of metal atom[26], geranium bimetallic lakes will not be considered in this study.

3.2.1. Synthesis of Pb-lakes

The results of the synthesis of Pb-lakes are displayed in Figure 6. The FTIR spectra of the obtained products show some variations (Figure 6, left side). On one hand, some products show a shoulder at ≈ 1450 cm^{-1} in the band at ≈ 1437 cm^{-1}, previously associated to the C=O symmetric stretching from the carboxylate group. Previous reports[51], have stablished a relationship between the position of the bands related to C=O symmetric and asymmetric stretching and the type of metal-carboxylate coordination. Specifically, if the distance between both bands in the complex is similar to the ionic compound (in this case the disodium salt of eosin Y, Figure 6c), the complex has bidentate bridging coordination, a bigger distance indicates an unidentate coordination and a smaller distance a bidentate chelating coordination. Therefore, since the C=O asymmetric stretching does not change (band at 1555 cm^{-1}), the peak at 1437 cm^{-1} is expected to be related to unidentate coordination and the shoulder at ≈ 1450 cm^{-1} suggests the formation of bidentate bridging coordination. The band at ≈ 1335 cm^{-1} (related to the phenoxide ion) shows shifts similar to the ones observed in the carboxylate group, i.e. a shoulder at 1344 cm^{-1}. This agrees with the hypothesis of a phenoxide ion-metal interactions previously mentioned: indeed, if this interaction takes place, a different coordination of the carboxylate-metal would affect the bands related to the phenoxide ion.

Thus, the FTIR spectra highlight a clear link between the coordination of the Pb-lakes and the synthesis conditions. If a larger amount of Pb(COOCH$_3$)$_2$ is used, the proportion of bidentate bridging coordinated complexes is higher, probably explained by the greater number of Pb^{2+} ions available in the solution. In a similar fashion, a higher pH$_i$ leads to a bigger proportion of bidentate bridging coordinated complexes, most likely because the proportion of eosin Y totally deprotonated is larger, so it has more electrons available to form more bonds with the metal.
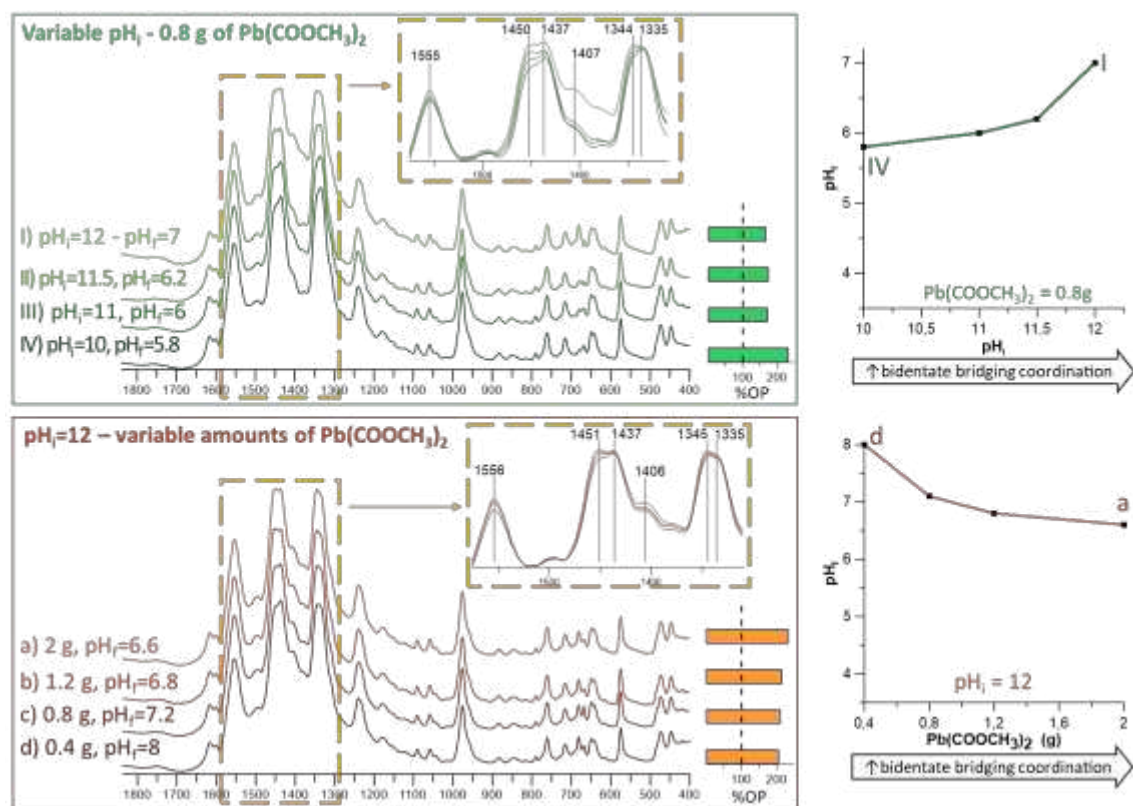
Figure 6. Synthesis of Pb-lake depending on the pH_i and the amount of $Pb(COOCH_3)_2$. Left: spectra of the compounds obtained with each type of synthesis, a magnification of the spectral region marked in yellow have been displayed. The %OP of each reaction is is presented in the bar plot at the right, using the chemical formula previously published[26]. Right: variations of the pH_f depending on the synthesis conditions. Top (green line): pH_f with different pH_i and $Pb(COOCH_3)_2=0.8g$, bottom (orange line): pH_f with different amount of $Pb(COOCH_3)_2$ and $pH_i=12$. The conditions that increase the proportion of bidentate bridging coordination are marked with an arrow.

The presence of by-products is linked to the shoulder at ≈ 1407 cm^{-1} since this band does not appear in the spectra of eosin Y, related compounds (Figures 4 and 5) or in the spectra of the metallic salts used for the synthesis (Figure S4). The amount of by-products formed strongly depends on the amount of metallic salt added, but also on the pH_f of the synthesis. This is due to the fact that the solubility of Pb salts is higher at lower pH[52,53], so the by-product formed is re-solubilized if the pH_f is low enough.

As it can be seen, the pH_f changes depending on the synthesis conditions (Figure 6, plots at the right). In general, when the metallic salt is added, in parallel to the formation of the eosin Y complex a reaction between OH$^-$ and Pb^{2+} takes place, leading to the precipitation of by-products and causing a diminution

20

1   of the pH. Hence, when the same amount of metallic salt is added, a lower pH_i results in a lower pH_f.

2   Consequently, the amount of by-product is smaller because it starts to solubilize (Figure 6, green spectra,

3   the peak at $\approx$1407 cm^{-1} related to the by-product decreases). Similarly, higher amounts of $Pb(COOCH_3)_2$

4   (Figure 6, orange spectra) result in lower pH_f, but also in a higher concentration of Pb^{2+} ions. Thus, the

5   effect of the solubilisation of the by-product at low pH is compensated by the larger amount of by-

6   product formed due to the higher amount of Pb^{2+} ions, consequently the final amount is analogous (peak

7   at $\approx$1407 cm^{-1} with similar intensity).

8   It may seem that a low pH_f is more convenient since this leads to a low amount of by-product, so the

9   obtained pigment is purer. However, it should be kept in mind that at low pH_f, eosin Y starts to protonate.

10   Indeed, the fraction of protonated eosin Y is too low to be detected in the FTIR spectra, however it can

11   be seen that at low pH_f the supernatant shows an orange tone (Figure S5), associated to the presence of

12   eosin Y. In any case, the pH_f does not decrease below 6-5.8 in all studied conditions, which is explained

13   by the equilibrium established by the by-products formed and the solubility of Pb^{2+} which increases at

14   low pH.[52,53]

15   Interestingly, the %OP of the Pb-lake synthesis (Figure 6, barplot) exceeds 100% in all cases, explained by

16   the presence of the by-product and the type of carboxylate-metal coordination. In fact, bidentate

17   bridging coordination means one atom of Pb per each ligand of eosin Y, which increases the total

18   molecular weight compared to the previous formula.[26] Consequently, a higher %OP is observed in the

19   compounds for which the spectra shows a bidentate bridging coordination.

20   Finally, other types of synthesis reported in the literature, with small variations in the procedure, have

21   been reproduced to verify if the results fit the trends previously observed (Figure S6).[26] These syntheses

22   start from a $Pb(COOCH_3)_2$ solution (pH_i =6.1), where eosin Y disodium salt is added, and from an eosin Y

23   disodium salt solution (pH_i =6.5), where the metallic salt is added. In the latter, two different amounts of

24     $Pb(COOCH_3)_2$ have been used to verify its influence. As it can be noticed, the predominant form is the

25   unidentate coordination, probably because the pH_i is too low and thus the proportion of deprotonated

1   eosin Y is limited. Therefore, the effect of pH is crucial: even adding high amounts of $Pb(COOCH_3)_2$, the

2   proportion of bidentate bridging coordination is lower compare to unidentate. Additionally, the synthesis

3   at very low pH_f has also been tested (spectrum d, Figure S6), by adding CH_3COOCH_3 to the final solution.

4   As it can be seen, the predominant coordination mode is unidentate. Eosin Y is surely mixed with the

5   obtained pigment but, unlike for Al-lakes, the bands cannot be seen in the spectra, due to the higher

6   molar absorptivity of Pb-lakes.

7

8   *3.2.2. Synthesis of Al-lakes*

9   The results of the synthesis of Al-lakes are displayed in Figure 7. The plots at the right showing the pH_f

10   depending on the synthesis conditions present the same trends seen for the Pb-lakes (Figure 6), i.e. the

11   pH_f is lower when pH_i is lower or when higher amounts of $Al_2(SO_4)_3$ are used. Like in the synthesis of Pb-

12   lakes, this is probably explained by the formation of a by-product of OH^- and Al^{3+}. However, the range of

13   pH_f obtained in the synthesis of Al-lakes, $pH_f \approx 3.7$, is lower and the range is narrower than in Pb-lake,

14   which can be explained by the lower solubility of the Al^{3+} salts[54] compared to Pb^{2+} salts[52]. Due to the lower

15   pH_f, a higher formation of protonated eosin Y is expected, which agrees with the colour of the

16   supernatants observed in all the performed experiments (Figure S5).

17   Regarding the characterization of the obtained products by FTIR spectroscopy (Figure 7, right side) no

18   shifts can be seen in the position of the bands related to the carboxylate group, therefore the metal-

19   carboxylate coordination does not change depending on the pH_f. Comparing the position of these bands

20   with the Pb-complex and the disodium salt of eosin Y, it can be assumed that the main metal-carboxylate

21   coordination of Al-lakes is bidentate bridging. However, since the band at 1448 cm^{-1} is quite broad, it is

22   feasible that other coordination modes exist in lower proportions and that the associated bands are

23   overlapped with the one at 1448 cm^{-1}. Besides the carboxylate bands, additional variations can be noticed

24   in other regions, namely I) the increase of the bands at 1753, 1503, 1205 and 1115 cm^{-1} and the shoulders

25   at $\approx$1570, 1418 and 1390 cm^{-1} at low pH_f, that can be related to the growing amount of protonated (i.e.

1   non-complexed) eosin Y, and II) the increase of broad bands at ≈ 1120 and ≈ 600 cm^{-1} at high pH$_f$, probably

2   associated to the presence of by-products of Al^{3+}. Likewise Pb-lakes, at low pH$_f$ a lower amount of by-

3   product and a higher amount of protonated eosin Y are generated.

4
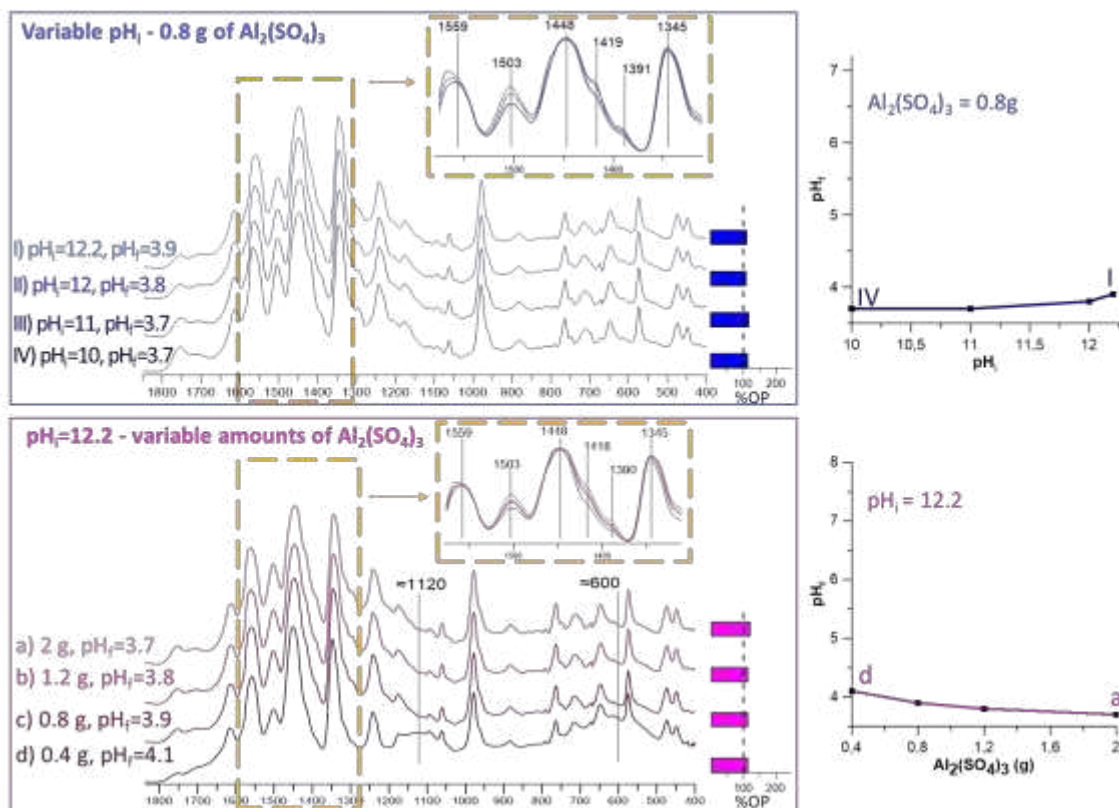
5

6   **Figure 7.** Synthesis of Al-lake depending on the pH$_i$ and the amount of Al$_2$(SO$_4$)$_3$. Left: spectra of the
7   compounds obtained with each type of synthesis using the same color code, a magnification of the
8   spectral region marked in yellow have been displayed. The %OP of each reaction is is presented In the
9   bar plot at the right, using the chemical formula previously published[26]. Right: variations of the pH$_f$
10   depending on the synthesis conditions. Top (blue line): pH$_f$ with different pH$_i$ and Al$_2$(SO$_4$)$_3$ =0.8g, bottom
11 (pink line): pH$_f$ with different amount of Al$_2$(SO$_4$)$_3$ and pH$_i$=12.2.

12

13 Regarding the %OP of the synthesis of Al-lake (Figure 7, barplot at the right), it can also be observed that

14 it is higher than 100%. Similar to Pb-lakes, this can be explained by the presence of by-products and by

15 the bidentate bridging coordination between the carboxylate and the metal, that would increase the

16 molecular weight of the lake. Compared to the Pb-lake, the %OP is smaller due to the lower atomic weight

1   of Al compared to Pb.

2   Additional experiments have also been performed in order to verify the effect of further small variations

3   in the synthesis protocol observed in the literature (Figure S7).[26] In the same fashion of Pb-lakes, the

4   conditions tested include to start the synthesis by a $Al_2(SO_4)_3$ solution (pH_i =3.3), where eosin Y disodium

5   salt is added, or by an eosin Y disodium salt solution (pH_i =6.5), where the metallic salt is added. In the

6   latter, two different amounts of $Al_2(SO_4)_3$ have been used to analyse its influence. As it can be seen, the

7   coordination of eosin Y-metal does not change. Indeed, the FTIR spectra seem very similar to the ones

8   obtained in Figure 7 with similar pH_f, meaning that Al-lakes form the bidentate bridging coordination

9   even when the proportion of deprotonated eosin Y is relatively low and independently of the amount of

10   metallic salt used. However, the proportion of eosin Y increases dramatically at low pH_f affecting severely

11   the purity of the obtained lake.

12   In conclusion, the carboxylate-metal coordination in Al-lakes is mostly bidentate bridging, while the

13   proportion of unidentate or bidentate bridging coordination in Pb-lakes depends on the synthesis

14   conditions. For the first time, the formation of by-products in both types of lakes has been demonstrated:

15   for Pb-lakes the amount of by-products decreases at low pH_f due to the increase of their solubility in

16   these conditions. In the case of Al-lakes, the by-products formed are less soluble and their amount is

17   significant even at the lowest pH_f tested. Additionally, protonated eosin Y is also found mixed with the

18   obtained lakes when the pH_f is low enough: its characteristic colour is noticeable in the supernatant at

19   pH_f <6 and in the related bands are distinguishable in the FTIR spectra at pH_f <4.

20   The different coordination modes of Pb-lakes may lead to differences in their reactivity, as it has been

21   previously demonstrated in other type of complexes[55,56]. Additionally, the presence of by-products and

22   eosin Y may also affect their chemical behaviour, especially since eosin Y degrades fast under specific

23   conditions[2]. Consequently, the type of synthesis of geranium lakes may affect its stability.

24   *3.3. Characterization of the by-products depending on the synthesis method*

25   The analysis of the FTIR spectra of geranium lakes allowed to link some of the bands to the co-

1 precipitation of by-products during the synthesis. The characterization of such by-products is of great

2 importance, since they might affect the purity of the pigments and, thus, their reactivity.

3 The behaviour of the metal solutions was separately investigated to characterize the by-products formed.

4 In detail, the same conditions used to synthesize Al- and Pb-lake were reproduced without the presence

5 of eosin Y in order to study the by-products formed depending on the pH. The obtained products have

6 been analysed by XRPD, FTIR and Raman spectroscopy.

7 The by-products generated by Pb salts are displayed in Figure 8. Two different products have been

8 detected depending on the pH_f: at pH_f >11 a pale yellow precipitate is formed, and at 11>pH_f >7 the

9 precipitate is white. Below pH=7 the precipitate starts to re-dissolve. At both pH, the FTIR (Figure 8, black

10 lines) and Raman (Figure 8, red lines) spectra show the spectral markers of lead (II) carbonate.[57] In

11 particular, the FTIR spectra of pH=8.2 suggests the presence of plumbonacrite ($Pb_5(CO_3)_3O(OH)_2$), due to

12 the presence of a band at 3430 and 865 cm^{-1} related to more than one site of OH$^-$ and CO_3^{2-}, respectively,

13 in the structure of the lead (II) carbonate. The presence of plumbonacrite is confirmed by the XRPD data

14 (Figure 8, green line), although the XRPD show an unidentified crystalline compound in the by-product at

15 pH=11.7. On the other hand, the XRPD analysis of the previously synthesized Pb-lakes (Figure 6) showed

16 the presence of another type of lead (II) carbonate, specifically hydrocerussite ($Pb_3(CO_3)_2(OH)_2$) (Figure

17 S8). This difference is probably explained by the lower amount of Pb^{2+} ions available during the synthesis,

18 since they are partially complexed to form the Pb-lake. The generated by-product re-dissolved

19 completely at pH<6.

20 The by-products generated by Al salts are displayed in Figure 9. In this case, all precipitates are white but

21 different spectral features have been observed at different pH_f. The FTIR spectra of the product obtained

22 at pH_f =9.1 shows the presence of bands related to amorphous basic aluminum carbonate[58], possibly

23 dawsonite[59]. At pH_f = 6.7 the spectrum is similar but the proportion of carbonate groups is lower since

24 the related bands (1528 and 1418 cm^{-1}) are less intense. Finally, at pH_f =3.5, the bands related to –OH

25 groups (3450 and 1650 cm^{-1}) are higher, indicating a higher proportion of this functionality. According to

1   the obtained spectra, the presence of basic aluminium sulphates at pH$_f$ = 6.7 and pH$_f$ = 3.5 is feasible.[60]

2   In this case, the XRPD diffractogram show no bands, in agreement with the amorphous nature of the

3   generated by-products, and the Raman spectra shows a broad band related to fluorescence, typically

4   seen in aluminium compounds. The generated by-product was insoluble at the lowest pH tested (pH=3.5).

5   The different solubility of the by-products agrees with the different pH$_f$ ranges observed for Pb-lakes and

6   Al-lakes.

7
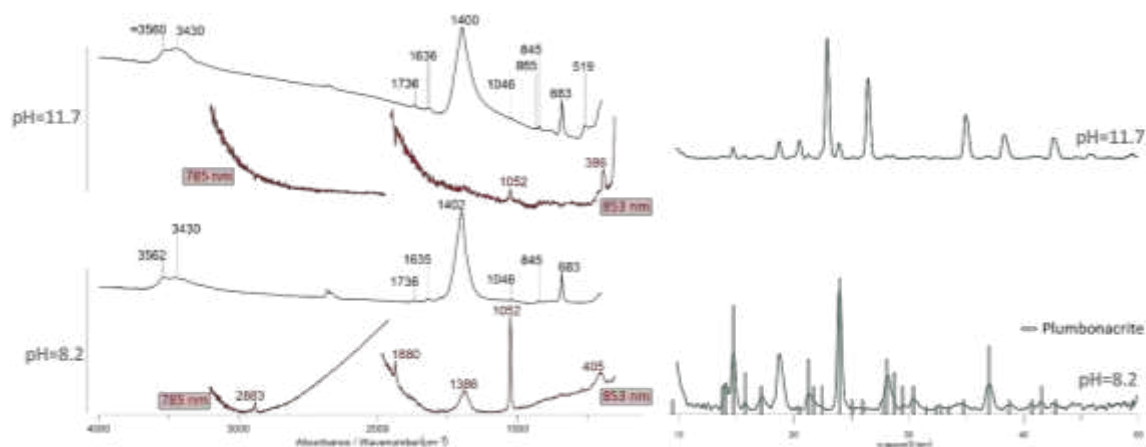
8

9   **Figure 8**. Spectra of the by-products obtained in the synthesis of Pb-lake at different pH (11.7 and 8.2).
10   Left: FTIR spectra are plotted in balck and Raman spectra in red (in order to avoid the fluorescence, two
11   wavelenghts were used, 785 nm and 853 nm). Right: XRD diffractograms are plotted in green compared
12   to the reference spectra of plumbonacrite (grey lines).

13

14   The presence of Pb and Al compounds can play an important role in the reactivity of the pigments used

15   in oil paintings. Lead carbonates are known to react with fatty acids from the binding media to produce

16   lead soaps, the formation of Al soaps has also been observed.[61–64] Metal soaps are associated with the

17   formation of protrusions and cracks in the paintings.[28] Thus, a higher proportion of these compounds

18   would cause a higher damage to the paintings, that should not be confused with the reactivity of

19   geranium lakes themselves. Furthermore, the presence of white by-products mixed with the complexes

20   might affect their long-term stability due to the scattering of the light, increasing their tendency to fade.

21   Lead carbonates mixed in the paint film, in particular, have been found to promote such fading process.[42]

1 Additionally, lead carbonates have been used in historical paintings as a white pigment, also in

2 combination with geranium lakes[11,14]. Knowing that such compounds could also exist as impurities in the

3 pigments is of great importance to accurately interpret and reconstruct the formulation of historical

4 paints. This is a relevant information to understand the artistic choices and the painting technique of the

5 artists who used these pigments, allowing to perform more accurate authentication and attribution of

6 paintings.

7
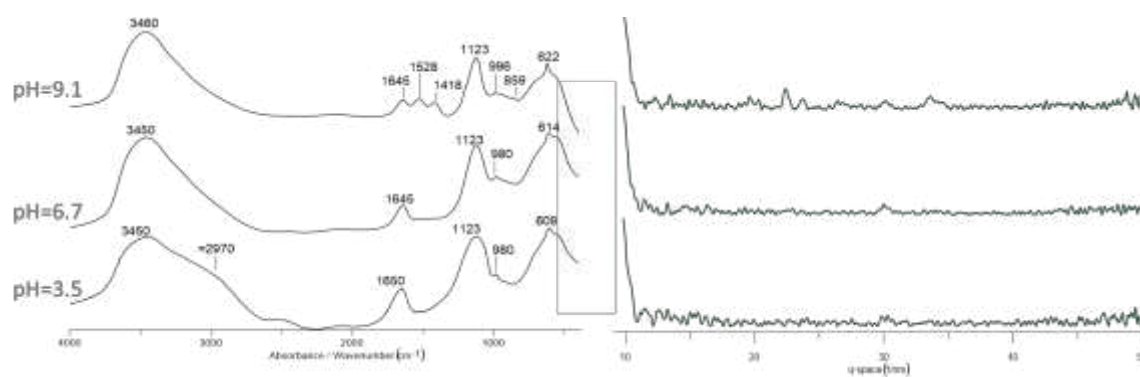
8

9 **Figure 9**. Left: FTIR spectra of the by-products obtained in the synthesis of Al-lake at different pH (9.1,
10 6.7 and 3.5). Right: XRD diffractograms (plotted in green).

11

12 **4. Conclusion**

13 This manuscript presents a thorough investigation of the structure and composition of eosin Y complexes

14 based in Al and Pb, by FTIR and Raman spectroscopies and complementary techniques, with a particular

15 focus on the effect of changes in the synthesis conditions.

16 In the first place, the results further the understanding of the eosin Y-metal coordination with Al and Pb,

17 showing a clear link between changes in the synthesis conditions and changes in such coordination. In

18 detail, Pb-lakes show an eosin Y-metal unidentate or a bidentate bridging coordination depending on pH_i

19 and amount of metallic salt used. Al-lakes, on the other hand, present mostly a bidentate bridging

20 coordination in all the synthesized products, nonetheless lower amounts of unidentate and bidentate

1 chelating coordination might also be present, as suggested by the broad C=O symmetric stretching band.

2 Furthermore, an additional interaction between the metal ion and the phenoxide ion, and thus the

3 xanthene moiety (chromophore), is proposed for all the complexes. This interaction is of capital

4 importance since it implies a potential influence of the metal ion on the properties of the fundamental

5 and excited states of the complexes, ultimately determining their reactivity. In addition, the evidence for

6 a chromophore-metal interaction presented in this study supports the literature findings on the

7 differences in colour and in reactivity for Al- and Pb-lakes.

8 In both cases, the synthesized lakes also contain by-products mixed with the eosin Y complexes. Such by-

9 products are detected and identified here for the first time. In detail, lead carbonates have been observed

10 in Pb-lake samples when the pH_f is higher than 6. Below this value, lead carbonates are not present due

11 to its solubility at low pH, however eosin Y starts to protonate and is found in the pigment powder. In the

12 case of Al-lakes, amorphous basic aluminium carbonate has been detected, with variable proportions of

13 carbonate and OH groups. Since the pH_f is low, around 3, the amount of eosin Y mixed with the

14 synthesized lake is higher than for the Pb-lakes. Consequently, the geranium lake pigments generated by

15 the synthesis methods studied will always contain impurities.

16 Additionally, a detailed band assignment of the FTIR and Raman spectra of eosin Y and Pb and Al-based

17 geranium lakes has been described. This band assignment has the potential to become a reference to

18 better understand and monitor molecular alterations during the degradation of geranium lakes and eosin

19 Y complexes in general, as well as to more easily distinguish these molecules in unknown samples.

20 This is of great importance not only for the analysis of historical paintings, but also for the study of any

21 other material containing eosin Y bonded to metallic ions. Particularly, in all the applications in which the

22 nature of the interaction between eosin Y and a metal/metal oxide surface could completely change the

23 outcome of a photochemical process, such as dye-sensitized solar cells, removal of dyes from

24 wastewater, or photocatalysis. The accurate characterization of the eosin Y complexes and by-products

25 discussed in this study will ultimately help to understand their reactivity.

1

5. Acknowledgements

6. Supplementary material description

The supplementary material includes additional results to support the conclusions.

7. Bibliographic references

(1)   Haugland, R. P. *Handbook of Fluorescent Probes and Research Products*; Molecular
        Probes: Paris, 2002.
(2)   Alvarez-martin, A.; Trashin, S.; Cuykx, M.; Covaci, A.; Wael, K. De; Janssens, K.
        Photodegradation Mechanisms and Kinetics of Eosin-Y in Oxic and Anoxic Conditions.
        Dye. Pigment. **2017**, *145*, 376–384.
(3)   Rahman, H. Utilization of Eosin Dye as an Ion Pairing Agent for Determination of
        Pharmaceuticals: A Brief Review. *Int. J. Pharm. Pharm. Sci.* **2017**, *9* (12), 1.
(4)   Derayea, S. M.; Nagy, D. M. Application of a Xanthene Dye, Eosin Y, as Spectroscopic
        Probe in Chemical and Pharmaceutical Analysis; a Review. *Rev. Anal. Chem.* **2018**, *37* (3),
        1–14.
(5)   Yoshida, T.; Iwaya, M.; Ando, H.; Oekermann, T.; Nonomura, K.; Schlettwein, D.; Wöhrle,
        D.; Minoura, H. Improved Photoelectrochemical Performance of Electrodeposited
        ZnO/EosinY Hybrid Thin Films by Dye Re-Adsorption. *Chem. Commun.* **2004**, *4* (4), 400–
        401.
(6)   Yoshida, T.; Terada, K.; Schlettwein, D.; Oekermann, T.; Sugiura, T.; Minoura, H.
        Electrochemical Self-Assembly of Nanoporous ZnO/Eosin Y Thin Films and Their
        Sensitized Photoelectrochemical Performance. *Adv. Mater.* **2000**, *12* (16), 1214–1217.
(7)   Hazebroucq, S.; Labat, F.; Lincot, D.; Adamo, C. Theoretical Insights on the Electronic
        Properties of Eosin Y, an Organic Dye for Photovoltaic Applications. *J. Phys. Chem. A*
        2008, *112* (31), 7264–7270.
(8)   Eastaugh, N.; Walsh, V.; Chaplin, T.; Siddal, R. *Pigment Compendium. A Dictionary and
        Optical Microscopy of Historical Pigments*; 2013; Vol. 53.
(9)   Gabrieli, F.; Doherty, B.; Miliani, C.; Degano, I.; Modugno, F.; Uldank, D.; Kunzelman, D.;
        Buzzegoli, E.; Patti, M.; Rosi, F. Micro-Raman and SER Spectroscopy to Unfold Lefranc's
        Early Organic Pigment Formulations. *J. Raman Spectrosc.* **2016**, *47* (12), 1505–1513.
(10)   *Van Gogh's Studio Practice*; Vellekoop Marije, Geldof Muriel, Hendriks Ella, Jansen Leo,
        de Tagle Alberto, Eds.; Mercatorfonds: Brussels, 2013.

(11) Distel, A.; Stein, S. A. *Cézanne to Van Gogh : The Collection of Doctor Gachet*; Metropolitan Museum of Art, 1999.

(12) Peres, C.; Hoyle, M.; Tilborgh, L. van. *A Closer Look : Technical and Art-Historical Studies on Works by Van Gogh and Gauguin*; Waanders Publishers: Zwolle, 1991.

(13) Geldof, M.; Proaño Gaibor, A. N.; Ligterink, F.; Hendriks, E.; Kirchner, E. Reconstructing Van Gogh's Palette to Determine the Optical Characteristics of His Paints. *Herit. Sci.* **2018**, *6* (1), 1–20.

(14) Centeno, S. A.; Hale, C.; Carò, F.; Cesaratto, A.; Shibayama, N.; Delaney, J.; Dooley, K.; van der Snickt, G.; Janssens, K.; Stein, S. A. Van Gogh's Irises and Roses: The Contribution of Chemical Analyses and Imaging to the Assessment of Color Changes in the Red Lake Pigments. *Herit. Sci.* **2017**, *5* (18), 1–11.

(15) Saunders, D.; Kirby, J. A Comparison of Light-Induced Damage under Common Museum Illuminants. In *ICOM Committee for Conservation, ICOM-CC, 15th Triennial Conference New Delhi, 22-26 September 2008: preprints*; Allied Publishers PVT: New Delhi, 2008; pp 766–774.

(16) Fieberg, J. E.; Knutås, P.; Hostettler, K.; Smith, G. D. "paintings Fade Like Flowers": Pigment Analysis and Digital Reconstruction of a Faded Pink Lake Pigment in Vincent van Gogh's Undergrowth with Two Figures. *Appl. Spectrosc.* **2017**, *71* (5), 794–808.

(17) Burnstock, A.; Lanfear, I.; van den Berg, K. J.; Carlyle, L.; Clarke, M.; Hendriks, E.; Kirby, J. Comparison of the Fading and Surface Deterioration of Red Lake Pigments in Six Paintings by Vincent van Gogh with Artificially Aged Paint Reconstructions. *ICOM-CC 14th Trienn. Conf. Prepr. Hague* **2005**, No. March 2017, 459–466.

(18) Alvarez-martin, A.; Janssens, K. Protecting and Stimulating e Ff Ect on the Degradation of Eosin Lakes . Part 1 : Lead White and Cobalt Blue. *Microchem. J.* **2020**, *141* (May 2018), 51–63.

(19) Chieli, A.; Miliani, C.; Degano, I.; Sabatini, F.; Tognotti, P.; Romani, A. New Insights into the Fading Mechanism of Geranium Lake in Painting Matrix". *Dye. Pigment.* **2020**, *181*, 108600.

(20) Sabatini, F.; Eis, E.; Degano, I.; Thoury, M.; Bonaduce, I.; Lluveras-tenorio, A. The Issue of Eosin Fading: A Combined Spectroscopic and Mass Spectrometric Approach Applied to Historical Lakes. *Dye. Pigment.* **2020**, *180*, 108436–108448.

(21) Claro, A.; Melo, M. J.; Schäfer, S.; de Melo, J. S. S.; Pina, F.; van den Berg, K. J.; Burnstock, A. The Use of Microspectrofluorimetry for the Characterization of Lake Pigments. *Talanta* **2008**, *74* (4), 922–929.

(22) Claro, A.; Melo, M. J.; Seixas de Melo, J. S.; van den Berg, K. J.; Burnstock, A.; Montague, M.; Newman, R. Identification of Red Colorants in van Gogh Paintings and Ancient Andean Textiles by Microspectrofluorimetry. *J. Cult. Herit.* **2010**, *11* (1), 27–34.

(23) Kirby, J. The Reconstruction of Late 19th-Century French Red Lake Pigments. In *Art of the Past: Sources and Reconstructions. Proceedings of the first symposium of the Art Technological Source Research study group*; Clarke, M., Townsend, J. H., Stijnman, A., Eds.; Archetype Publications: London, 2005.

(24) Vanzin, D.; Freitas, C. F.; Pellosi, D. S.; Batistela, V. R.; Machado, A. E. H.; Pontes, R. M.; Caetano, W.; Hioka, N. Experimental and Computational Studies of Protolytic and Tautomeric Equilibria of Erythrosin B and Eosin y in Water/DMSO. *RSC Adv.* **2016**, *6* (111), 110312–110328.

(25) Schweitzer, C.; Schmidt, R. Physical Mechanisms of Generation and Deactivation of Singlet Oxygen. *Chem. Rev.* **2003**, *103* (5), 1685–1758.

(26) Anselmi, C.; Capitani, D.; Tintaru, A.; Doherty, B.; Sgamellotti, A.; Miliani, C. Beyond the Color: A Structural Insight to Eosin-Based Lakes. *Dye. Pigment.* **2017**, *140*, 297–311.

(27) van den Berg, K. J.; Burnstock, A.; Carlyle, L.; Clarke, M.; Hendriks, E.; Hoppenbrouwers, R.; Kirby, J.; Lanfear, I. Fading of Red Lake Paints after Vincent van Gogh - an Interdisciplinary Study Involving Three De Mayerne Projects. *Report. Highlights Mayerne Program.* **2006**, 89–96.

(28) *Metal Soaps in Art. Conservation and Research*; Casadio, F., Keune, K., Hendriks, E., Centeno, S. A., Eds.; Springer International Publishing, 2019.

(29) Amat-Guerri, F.; López-González, M. M. C.; Martínez-Utrilla, R.; Sastre, R. Synthesis and Spectroscopic Properties of New Rose Bengal and Eosin Y Derivatives. *Dye. Pigment.* **1990**, *12* (4), 249–272.

(30) Lamberts, J. J. M.; Neckers, D. C. Rose Bengal and Non-Polar Derivatives: The Birth of Dye Sensitizers for Photooxidation. *Zeitschrift für Naturforsch. B* **2014**, *39* (4), 474–484.

(31) Markuszewski, R.; Diehl, H. The Infrared Spectra and Structures of the Three Solid Forms of Fluorescein and Related Compounds. *Talanta* **1980**, *27* (11), 937–946.

(32) Greeneltch, N. G.; Davis, A. S.; Valley, N. A.; Casadio, F.; Schatz, G. C.; Van Duyne, R. P.; Shah, N. C. Near-Infrared Surface-Enhanced Raman Spectroscopy (NIR-SERS) for the Identification of Eosin Y: Theoretical Calculations and Evaluation of Two Different Nanoplasmonic Substrates. **2012**.

(33) Watanabe, H.; Hayazawa, N.; Inouye, Y.; Kawata, S. DFT Vibrational Calculations of Rhodamine 6G Adsorbed on Silver: Analysis of Tip-Enhanced Raman Spectroscopy. **2005**.

(34) Bellamy, L. *The Infra-Red Spectra of Complex Molecules.*; 1975.

(35) Lin-Vien, D.; Colthup, N. B.; Fateley, W. G.; Grasselli, J. G. (Professor). *The Handbook of Infrared and Raman Characteristic Frequencies of Organic Molecules*; Academic Press, 1991.

(36) Majoube, M.; Henry, M. Fourier Transform Raman and Infrared and Surface-Enhanced Raman Spectra for Rhodamine 6G. *Spectrochim. Acta Part A Mol. Spectrosc.* **1991**, *47* (9–10), 1459–1466.

(37) Wang, L.; Roitberg, A.; Meuse, C.; Gaigalas, A. K. Raman and FTIR Spectroscopies of Fluorescein in Solutions. *Spectrochim. Acta - Part A Mol. Biomol. Spectrosc.* **2001**, *57* (9), 1781–1791.

(38) Davies, M.; Jones, R. L. Infra-Red Absorptions and Molecular Structures of Phenol, Phenolphthalein, Fluorescein, and Some Alkali Derivatives. *J. Chem. Soc.* **1954**, No. 0, 120–125.

(39) Aronson, M.; Beckmann, P.; Ross, B.; Tan, S. L. Intramolecular Reorientations and the Effects of Thermal History and Hydrogen Bonding in Four Closely Related Organic Molecular Solids. *Chem. Phys.* **1981**, *63* (3), 349–358.

(40) Pouchert, C. *Aldrich Library of FT-IR Spectra*; The Aldrich Library of FT-IR Spectra; Wiley: Milwaukee, 1989.

(41) Wysocki, L. M.; Lavis, L. D. Advances in the Chemistry of Small Molecule Fluorescent Probes. *Current Opinion in Chemical Biology*. Elsevier Ltd December 1, 2011, pp 752–759.

(42) Alvarez-Martin, A.; Janssens, K. Protecting and Stimulating Effect on the Degradation of

Eosin Lakes. Part 1: Lead White and Cobalt Blue. *Microchem. J.* **2018**, *141* (September 2017), 51–63.

(43) Zhang, F.; Shi, F.; Ma, W.; Gao, F.; Jiao, Y.; Li, H.; Wang, J.; Shan, X.; Lu, X.; Meng, S. Controlling Adsorption Structure of Eosin y Dye on Nanocrystalline TiO 2 Films for Improved Photovoltaic Performances. *J. Phys. Chem. C* **2013**, *117* (28), 14659–14666.

(44) Mehandzhiyski, A. Y.; Riccardi, E.; Van Erp, T. S.; Koch, H.; Åstrand, P. O.; Trinh, T. T.; Grimes, B. A. Density Functional Theory Study on the Interactions of Metal Ions with Long Chain Deprotonated Carboxylic Acids. *J. Phys. Chem. A* **2015**, *119* (40), 10195–10203. h

(45) Bellamy, L. J.; Branch, R. F. The Infra-Red Spectra of Chelate Compounds. Part II. Metal Chelate Compounds of p -Diketones and of Salicylaldehyde. *J. Chem. Soc.* **1954**, 4491–4494.

(46) Nishikiori, H.; Uesugi, Y.; Takami, S.; Setiawan, R. A.; Fujii, T.; Qian, W.; El-Sayed, M. A. Influence of Steam Treatment on Dye-Titania Complex Formation and Photoelectric Conversion Property of Dye-Doped Titania Gel. *J. Phys. Chem. C* **2011**, *115* (6), 2880–2887.

(47) Alvarez-Martin, A.; Cleland, T. P.; Kavich, G. M.; Janssens, K.; Newsome, G. A. Rapid Evaluation of the Debromination Mechanism of Eosin in Oil Paint by Direct Analysis in Real Time and Direct Infusion-Electrospray Ionization Mass Spectrometry. *Anal. Chem.* **2019**, *91* (16), 10856–10863.

(48) Alwin, S.; Sahaya Shajan, X.; Menon, R.; Nabhiraj, P. Y.; Warrier, K. G. K.; Mohan Rao, G. Surfacemodification of Titania Aerogel Films by Oxygen Plasma Treatment for Enhanced Dye Adsorption. *Thin Solid Films* **2015**, *595*, 164–170.

(49) Narayanan, V. A.; Stokes, D. L.; Vo-Dinh, T. Vibrational Spectral Analysis of Eosin Y and Erythrosin B-Intensity Studies for Quantitative Detection of the Dyes. *J. Raman Spectrosc.* **1994**, *25* (6), 415–422.

(50) Azmi, S. N. H.; Al-Fazari, A.; Al-Badaei, M.; Al-Mahrazi, R. Utility of Eosin Y as a Complexing Reagent for the Determination of Citalopram Hydrobromide in Commercial Dosage Forms by Fluorescence Spectrophotometry. *Luminescence* **2015**, *30* (8), 1352–1359.

(51) Nakamoto, K. *Infrared and Raman Spectra of Inorganic and Coordination Compounds*, 3rd ed.; Wiley: New York, 1978.

(52) Keim, M. F.; Gassmann, B.; Markl, G. Formation of Basic Lead Phases during Fire-Setting and Other Natural and Man-Made Processes. *Am. Mineral.* **2017**, *102* (7), 1482–1500.

(53) Bilinski, H.; Schindler, P. Solubility and Equilibrium Constants of Lead in Carbonate Solutions (25°C, I = 0.3 Mol Dm-3). *Geochim. Cosmochim. Acta* **1982**, *46* (6), 921–928.

(54) Kvech, S.; Edwards, M. Solubility Controls on Aluminum in Drinking Water at Relatively Low and High PH. *Water Res.* **2002**, *36* (17), 4356–4368. https://doi.org/10.1016/S0043-1354(02)00137-9.

(55) Farrell, N.; Qu, Y.; Feng, L.; Van Houten, B. Comparison of Chemical Reactivity, Cytotoxicity, Interstrand Cross-Linking and DNA Sequence Specificity of Bis(Platinum) Complexes Containing Monodentate or Bidentate Coordination Spheres with Their Monomeric Analogues. *Biochemistry* **1990**, *29* (41), 9522–9531.

(56) Ducháčková, L.; Schröder, D.; Roithová, J. Effect of the Carboxylate Shift on the Reactivity of Zinc Complexes in the Gas Phase. *Inorg. Chem.* **2011**, *50* (7), 3153–3158.

1 (57) Siidra, O.; Nekrasova, D.; Depmeier, W.; Chukanov, N.; Zaitsev, A.; Turner, R.
2   Hydrocerussite-Related Minerals and Materials: Structural Principles, Chemical
3   Variations and Infrared Spectroscopy. *Acta Crystallogr. Sect. B Struct. Sci. Cryst. Eng.*
4   *Mater.* **2018**, *74* (2), 182–195.
5 (58) Contreras, C. A.; Sugita, S.; Ramos, E. Preparation of Sodium Aluminate From Basic
6   Aluminium Sulfate. *Adv. Technol. Mater. Mater. Process. J.* **2006**, *2* (8), 122–129.
7 (59) Schaller, R. F.; Jove-Colon, C. F.; Taylor, J. M.; Schindelholz, E. J. The Controlling Role of
8   Sodium and Carbonate on the Atmospheric Corrosion Rate of Aluminum. *npj Mater.*
9   *Degrad.* **2017**, *1* (1), 1–8.
10 (60) Zamorategui Molina, A.; del Ángel Soto, J.; Martínez Rosales, M.; Romero Toledo, R.
11   Ammonium Alunite and Basic Aluminum Sulfate: Effect of Precipitant Agent. *Int. J.*
12   *Mater. Sci. Appl.* **2015**, *4* (2), 100.
13 (61) Ma, X.; Beltran, V.; Ramer, G.; Pavlidis, G.; Parkinson, D. Y.; Thoury, M.; Meldrum, T.;
14   Centrone, A.; Berrie, B. H. Revealing the Distribution of Metal Carboxylates in Oil Paint
15   from the Micro- to Nanoscale. *Angew. Chemie Int. Ed.* **2019**.
16 (62) Spring, M.; Ricci, C.; Peggie, D. A.; Kazarian, S. G. ATR-FTIR Imaging for the Analysis of
17   Organic Materials in Paint Cross Sections: Case Studies on Paint Samples from the
18   National Gallery, London. *Anal. Bioanal. Chem.* **2008**, *392* (1–2), 37–45.
19 (63) Salvadó, N.; Butí, S.; Nicholson, J.; Emerich, H.; Labrador, A.; Pradell, T. Identification of
20   Reaction Compounds in Micrometric Layers from Gothic Paintings Using Combined SR-
21   XRD and SR-FTIR. *Talanta* **2009**, *79* (2), 419–428.
22 (64) Cotte, M.; Checroun, E.; De Nolf, W.; Taniguchi, Y.; De Viguerie, L.; Burghammer, M.;
23   Walter, P.; Rivard, C.; Salomé, M.; Janssens, K.; Susini, J. Lead Soaps in Paintings: Friends
24   or Foes? *Stud. Conserv.* **2017**, *62* (1), 2–23.

25

26

27

1   **Geranium lake pigments: the role of the synthesis on the structure and composition**

2   Victoria Beltran[1,2]*, Andrea Marchetti[1,2]*, Steven De Meyer[1,2], Gert Nuyts[1,2], Karolien De Wael[1,2+]

3   [1]AXES research group, University of Antwerp, Groenenborgerlaan 171, 2020, Antwerp, Belgium

4   [2]NanoLab Center of Excellence, University of Antwerp, Groenenborgerlaan 171, 2020, Antwerp,
5   Belgium.

6   * These authors contributed equally to this work

7   + corresponding author: karolien.dewael@uantwerpen.be

8

Supplementary Material
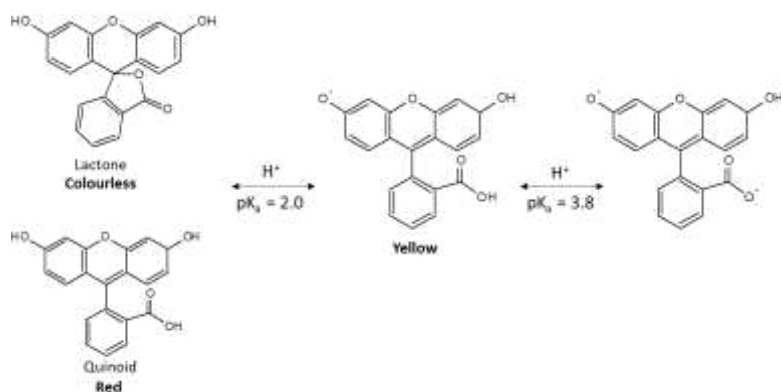
10

11   **Figure S1**. Main tautomers and pK$_a$ of fluorescein. The colors based in previous literature[1]
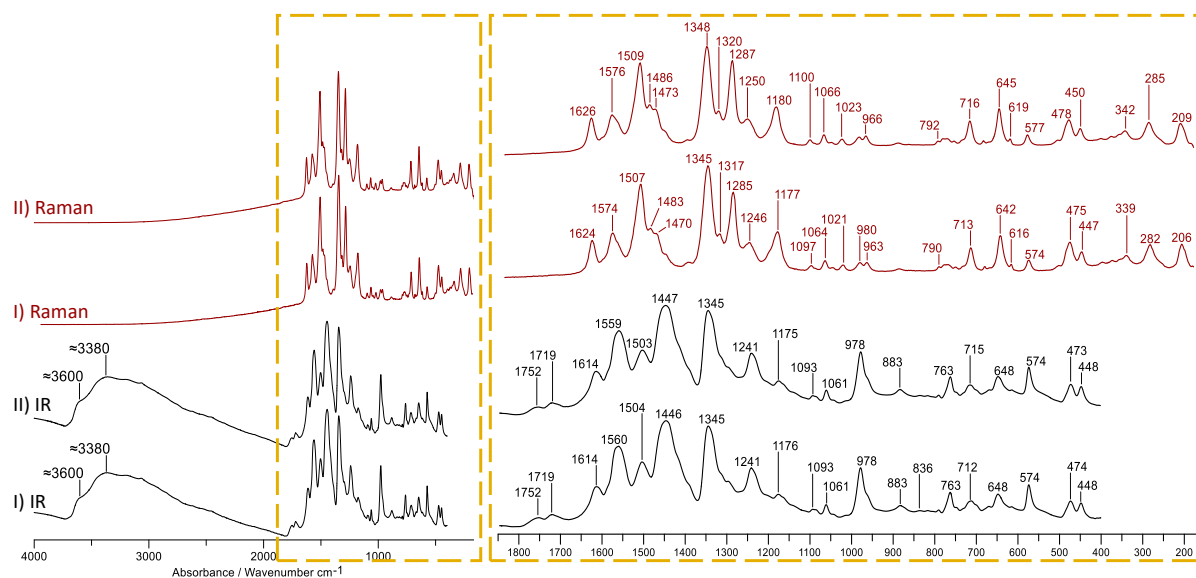
12

13   **Figure S2**. Raman and FTIR spectra of aluminum based geranium lakes prepared with I) Al$_2$(SO$_4$)$_3$ and II)
14   AlCl$_3$. A magnification of the spectral region marked in yellow have been displayed

15

Pb-lake	Al-lake
pH$_i$ = 12 0.8 g Pb(Ac)$_2$	pH$_i$ = 12 0.8 g Al$_2$(SO$_4$)$_3$
pH$_f$ = 4.6	*pH$_f$ = 3.9*
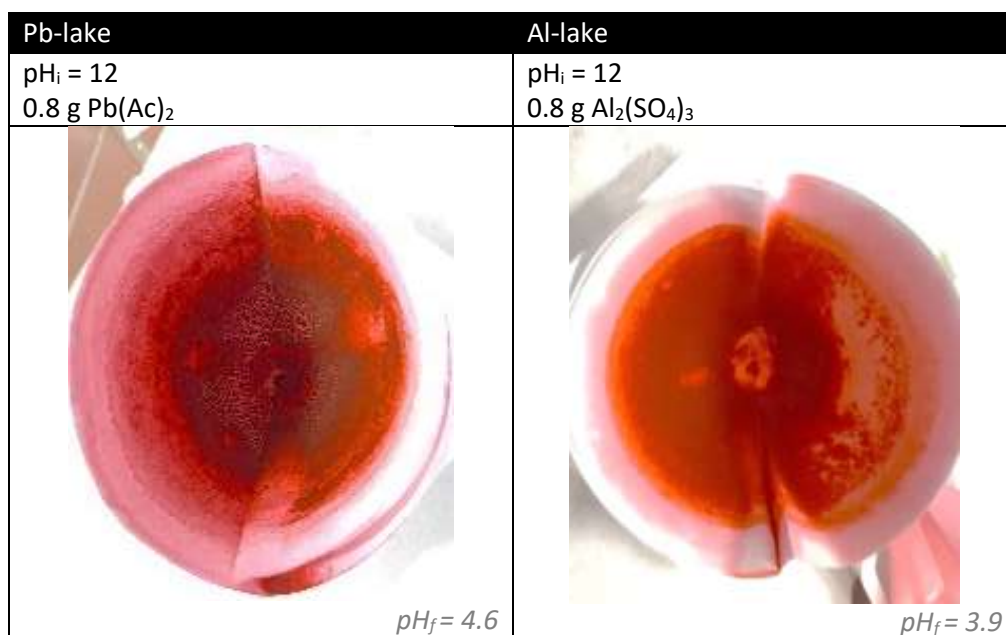
Figure S3. Color of Pb-lake and Al-lake obtained at similar synthesis conditions.
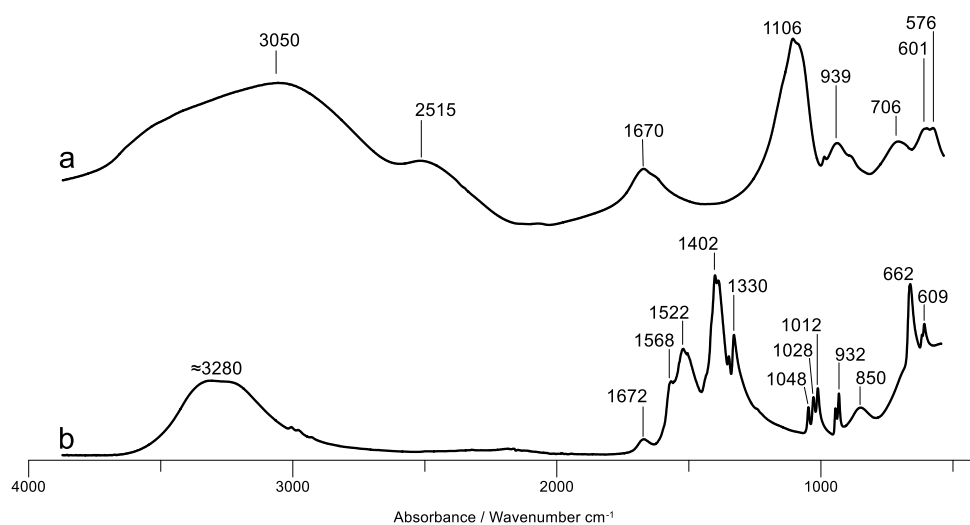
Figure S4. FTIR spectra of the metallic salts used to prepare the complexes a) Al$_2$(SO$_4$)$_3$ and b) Pb(COOCH$_3$)$_2$

0.8 g Pb(Ac)$_2$			
pH$_i$ = 12	pH$_i$ = 11.5	pH$_i$ = 11	pH$_i$ = 10
pH$_f$ = 7	pH$_f$ = 6.2	pH$_f$ = 6	pH$_f$ = 5.8

Pb-lake

pH$_i$ = 12			
0.4 g Pb(Ac)$_2$	0.8 g Pb(Ac)$_2$	1.2 g Pb(Ac)$_2$	2 g Pb(Ac)$_2$
pH$_f$ = 8	pH$_f$ = 7.2	pH$_f$ = 6.8	pH$_f$ = 6.6

Pb-lake

0.8 g Al$_2$(SO$_4$)$_3$			
pH$_i$ = 12.2	pH$_i$ = 12	pH$_i$ = 11	pH$_i$ = 10
pH$_f$ = 3.9	pH$_f$ = 3.8	pH$_f$ = 3.7	pH$_f$ = 3.7

Al-lake

pH$_i$ = 12			
0.4 g Al$_2$(SO$_4$)$_3$	0.8 g Al$_2$(SO$_4$)$_3$	1.2 g Al$_2$(SO$_4$)$_3$	2 g Al$_2$(SO$_4$)$_3$
pH$_f$ = 4.1	pH$_f$ = 3.9	pH$_f$ = 3.8	pH$_f$ = 3.7

Al-lake

Figure S5. Filtered supernatant of Pb-lake and Al-lake synthesis depending on the conditions.
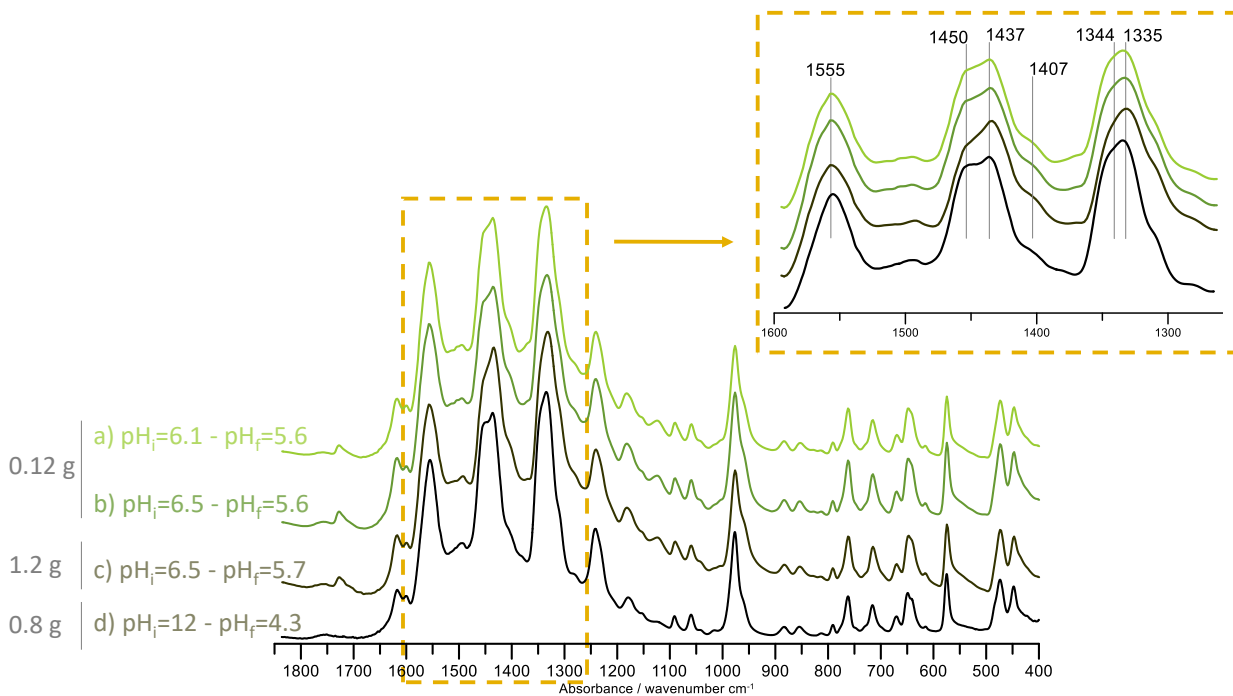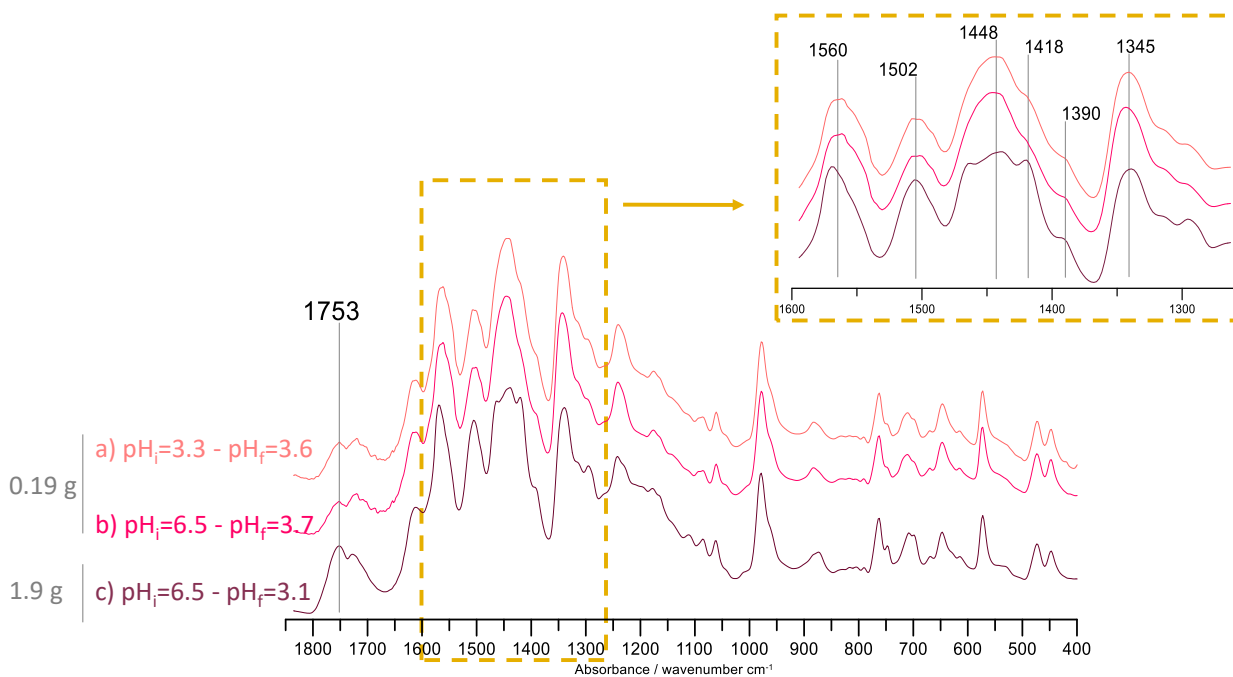
Figure S6. FTIR spectra of the Pb-lakes obtained at other type of conditions. A magnification of the spectral region marked in yellow is displayed.
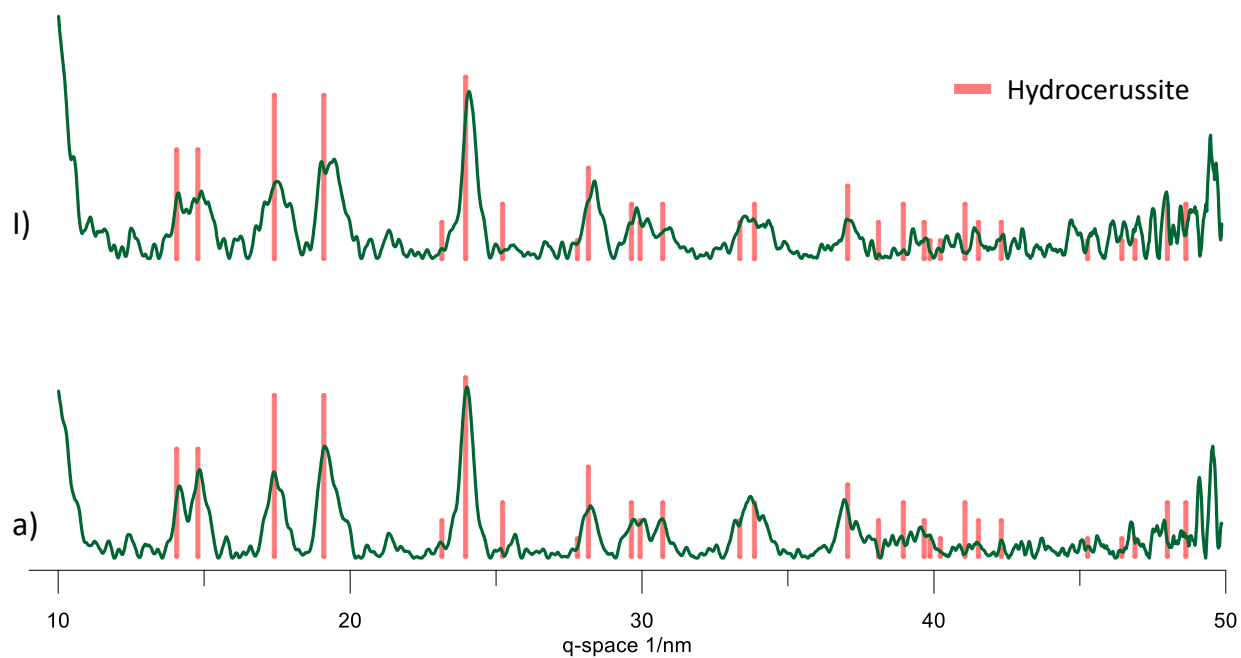

Figure S7. FTIR spectra of the Al-lakes obtained at other type of conditions. A magnification of the spectral region marked in yellow is displayed.

Figure S8. XRD diffractograms of the Pb-lakes synthesized in Figure 6 corresponding to spectra I) and a). The graphs have been compared to reference spectra of hydrocerussite (pink lines).

References

(1)   Markuszewski, R.; Diehl, H. The Infrared Spectra and Structures of the Three Solid Forms of Fluorescein and Related Compounds. *Talanta* **1980**, *27* (11), 937–946.